MetaGen: A DSL, Database, and Benchmark for VLM-Assisted Metamaterial Generation

Liane Makatura[*] MIT CSAIL
Benjamin Jones[*] MIT CSAIL
Siyuan Bian Shanghai Jiao Tong University
Wojciech Matusik MIT CSAIL

Abstract

Metamaterials are micro-architected structures whose geometry imparts highly tunable—often counter-intuitive—bulk properties. Yet their design is difficult because of geometric complexity and a non-trivial mapping from architecture to behaviour. We address these challenges with three complementary contributions. **(i)** ***MetaDSL***: a compact, semantically rich domain-specific language (DSL) that captures diverse metamaterial designs in a form that is human-readable and machine-parsable. **(ii)** ***MetaDB***: a curated repository of more than $150\,000$ parameterized MetaDSL programs together with their derivatives—three-dimensional geometry, multi-view renderings, and simulated elastic properties. **(iii)** ***MetaBench***: benchmark suites that test three core capabilities of vision–language metamaterial assistants—structure reconstruction, property-driven inverse design, and performance prediction. We establish baselines by fine-tuning state-of-the-art vision–language models and deploy an omni-model within an interactive, CAD-like interface. Case studies show that our framework provides a strong first step toward integrated design and understanding of structure–representation–property relationships.

1 Introduction

Metamaterials represent a key frontier in materials science: by exploiting small, patterned geometries, they endow bulk materials with properties beyond those of the constituent substance. Careful geometric tuning yields extraordinary behaviours such as programmable deformation [Jenett et al., 2020, Babaee et al., 2013], extreme strength-to-weight ratios [Qin et al., 2017], and materials that are both stiff and stretchy [Surjadi et al., 2025]. The design space is effectively limitless, with exciting applications ranging from thermal management [Fan et al., 2022, Attarzadeh et al., 2022] to biomedical implants [Ataee et al., 2018, Ambu and Morabito, 2019].

Despite this promise, neither the design nor the downstream adoption of metamaterials have realized their full potential. This is largely due to three long-standing hurdles: (i) navigating the immense geometric diversity of candidate architectures; (ii) characterizing the intricate structure–property relationship; and (iii) collating information and assets from the highly-fragmented literature base, which spans several fields and exhibits considerable variation in terminology, goals, assumptions, geometry descriptors, and evaluation protocols [Makatura et al., 2023, Lee et al., 2024, Xue et al., 2025, Surjadi and Portela, 2025]. These hurdles create a consistently high barrier to entry.

Vision–language models (VLMs) are poised to address this, as they excel at the cross-modal reasoning, retrieval, and generation required for effective metamaterial design – spanning text, images, 3-D geometry, and numerical property vectors. VLMs could also democratize metamaterial design by exposing a unified knowledge base through natural, conversational formats. Unfortunately, due to the hurdles discussed above, high-quality data curation presents a significant barrier for VLM training and more general data-driven metamaterial design approaches [Lee et al., 2024].

[*]Equal contribution

To address this issue, we introduce a general, extensible ecosystem for AI-assisted metamaterial design, anchored by 3 components:

1. **MetaDSL**: a domain-specific language (DSL) that captures metamaterials in a structured, compact, and expressive form accessible to both humans and VLMs.
2. **MetaDB**: a database of more than 150 000 metamaterials, each of which pairs a MetaDSL program with the derived 3-D geometry, rendered images, and simulated properties.
3. **MetaBench**: benchmark suites that probes three fundamental metamaterial design tasks – structure reconstruction, property-driven inverse design, and performance prediction – using data sampled from MetaDB.

To complete our vision, we use MetaBench to train and evaluate *MetaAssist*, a VLM assistant baseline and interactive CAD environment that facilitates multi-modal design interactions including language, images, geometry, and MetaDSL code.

All four components are designed for extensibility and community contribution, such that they can evolve seamlessly alongside the state of the art in materials science and agentic design. Collectively, our ecosystem provides a coherent, extensible knowledge base for metamaterial design, while laying the foundation for intuitive, efficient human–AI collaboration in architected materials.

2 Background

Metamaterials Experts commonly use forward design to craft parameterized structures for specific targets [Muhammad and Lim, 2021, Frenzel et al., 2017, Meier et al., 2025]. Inverse design approaches [Lee et al., 2024] are often driven by data-informed search over particular shape representation sweeps. Panetta et al. [2015] analysed 1205 families of cubic truss lattices, while Abu-Mualla and Huang [2024] expanded to 17 000 truss structures spanning six crystal lattices. High-throughput workflows also consider thousands of thin-shell architectures including plate lattices [Sun et al., 2023a] and TPMS-inspired surfaces [Xu et al., 2023, Liu et al., 2022, Yang and Buehler, 2022, Chan et al., 2020]. Because many datasets target a single architecture class (e.g. beams or shells) and a narrow performance metric, they restrict the attainable property gamut and thus the capability of downstream models [Berger et al., 2017, Lee et al., 2024]. Recent designs also increasingly blend classes in hybrid or hierarchical forms [Surjadi et al., 2025, Chen et al., 2019, White et al., 2021], emphasizing the need for representations that span such boundaries. The procedural-graph approach of Makatura et al. [2023] captures diverse geometries but is demonstrated primarily for human-in-the-loop workflows. Voxel and hybrid encodings scale to 140 k–180 k diverse structures [Yang et al., 2024a, Xue et al., 2025], but they sacrifice semantic clarity and compactness, which complicates human or agent editing. Such tradeoffs – along with inconsistencies in geometry descriptors, vocabularies, and evaluation protocols – continue to impede dataset reuse and extensibility [Lee et al., 2024]. We close these gaps with a universal metamaterial descriptor (MetaDSL) along with a reconfigurable database of 150 000 metamaterials (MetaDB). Each MetaDB entry couples a succinct, semantically rich program with derived 3-D geometry, renderings, and simulated properties, enabling consistent comparison and seamless expansion. Programmatic templating further enlarges the design space, and community contributions can grow both MetaDB and the accompanying benchmark suite.

Vision–Language Models for Design Vision–language models (VLMs) have permeated design tasks, including procedural textures [Li et al., 2025], 3-D scenes [Yang et al., 2024b, Kumaran et al., 2023], mesh generation and editing [Sun et al., 2023b, Wang et al., 2024, Jones et al., 2025, Huang et al., 2024, Yamada et al., 2024], interior layouts [Çelen et al., 2024], sewing-pattern synthesis [Nakayama et al., 2025, Bian et al., 2025], and computer-aided engineering and manufacturing [Makatura et al., 2024a,b, Choi et al., 2025, Yuan et al., 2024]. In most cases, code serves as the medium: pretrained models follow instructions, reuse standard patterns, and emit domain-specific scripts (e.g. Blender Python). When tasks demand novel grammars or specialist knowledge, fine-tuning further elevates performance [Zhou et al., 2025]. Our work adopts this code-centric philosophy but tailors it to metamaterials, whose design demands rich geometric semantics, physical constraints, and fluid translation among text, images, programs, and numerical property vectors. By grounding the interface in a purpose-built DSL and a physically validated database, we lay a robust foundation for future VLMs to reason about, generate, and refine architected materials at scale.

```
1  from metagen import *
2
3  def make_structure( shell_thickness : float =0.03) -> Structure :
4      v0 = vertex (cuboid.edges.FRONT_LEFT)                                  # (a) build skeleton over cuboid CP
5      v1 = vertex (cuboid.edges.FRONT_RIGHT)
6      v2 = vertex (cuboid.edges.BOTTOM_RIGHT, [0.4])
7      v3 = vertex (cuboid. faces .BOTTOM, [0.3, 0.3])
8      v4 = vertex (cuboid.edges.BOTTOM_RIGHT, [0.2])
9      v5 = vertex (cuboid.edges.BACK_RIGHT)
10     v6 = vertex (cuboid.edges.BACK_LEFT)
11     v7 = vertex (cuboid.edges.TOP_LEFT, [0.6])
12     v8 = vertex (cuboid. faces .TOP, [0.7,  0.7])
13     v9 = vertex (cuboid.edges.TOP_LEFT, [0.8])
14
15     c0 = Polyline ([v0, v1])
16     c1 = Curve([v1, v2, v3, v4, v5])
17     c2 = Polyline ([v5, v6])
18     c3 = Curve([v6, v7, v8, v9, v0])
19
20     skel = skeleton ([c0, c1, c2, c3])
21     shell = UniformTPMSShellViaMixedMinimal(skel, shell_thickness)         # (b) select lifting procedure
22
23     widthLtoR = 0.25                                                        # (c) define and apply embedding
24     heightTtoB = 0.25
25     depthFtoB = 0.5
26     embedding = cuboid.embed(widthLtoR, heightTtoB, depthFtoB, cornerAtAABBMin=cuboid.corners.BACK_BOTTOM_RIGHT)
27     tile = Tile ([ shell ], embedding)
28
29     pat = Custom(Mirror(cuboid.faces .TOP, True,                            # define the pattern
30                      Mirror(cuboid. faces .TOP, True,
31                         Mirror(cuboid. faces .LEFT, True,
32                            Mirror(cuboid. faces .LEFT, True,
33                               Rotate180([cuboid.edges.FRONT_LEFT, cuboid.edges.FRONT_RIGHT], True))))))
34     obj = Structure ( tile , pat)                                           # (d) apply the pattern
35
36     return obj
```

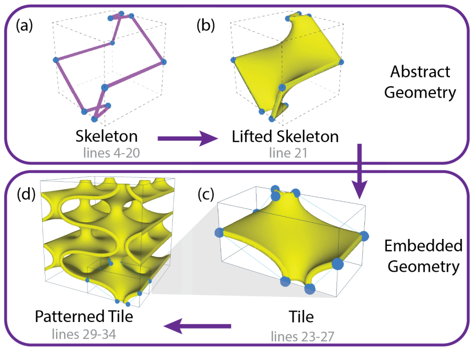

Figure 1: **(Left)** A MetaDSL program, and **(Right)** illustrations of each construction stage (clockwise): **(a)** build a skeleton relative to an abstract convex polytope, Π_{abs} – here, a cuboid; **(b)** specify the procedure lifting the skeleton to a 3D volume; **(c)** create a tile by embedding Π_{abs} in $\mathbb{R}^3$ and executing the lifting procedure; and finally, **(d)** tessellate the tile according to the specified pattern.

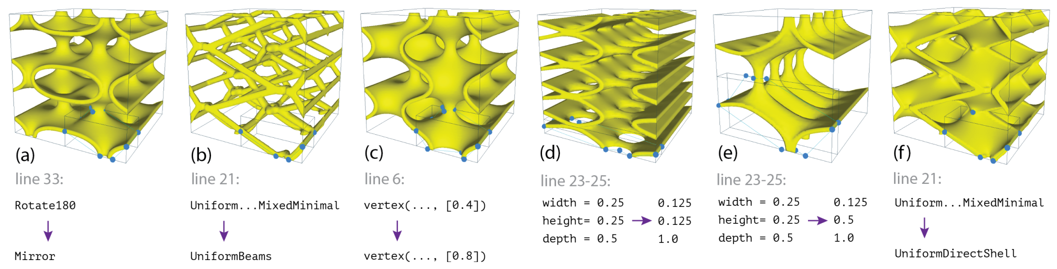

Figure 2: We illustrate the expressive power of MetaDSL by showing six different structures that all stem from the program shown in Figure 1(a). Each one is produced by changing a single aspect of the original program, as detailed below each structure.

3 Domain-Specific Language

Metamaterial design hinges on precise, expressive geometry representation, but the representational demands (RD) increase dramatically in service of a unified, extensible ecosystem. To dynamically serve both humans and computational agents, our metamaterial representation must be: (RD1) expressive, to support the full range of architectures; (RD2) modular and reconfigurable; (RD3) compact, semantically meaningful, and easy to use; (RD4) amenable to and robust under generative design; (RD5) verifiable and valid-by-construction and (RD6) flexible, to support experimentation and extensions. MetaDSL lays out a long-term design philosophy uniquely amenable to these goals. Our current implementation tackles a core subset (Section 3.2), but our infrastructure is purposefully extensible. This will facilitate the evolution of MetaDSL, such that new design paradigms can be added as metamaterial research matures, without invalidating existing programs.

3.1 Language Design Philosophy

MetaDSL uses a modular, compositional approach supported by a rich type system that determines compatibility between components. This promotes flexibility while ensuring verifiable outcomes. As shown in Figure 1, our highest-level decomposition mimics a hierarchical approach that is common in metamaterial design: *tiles* are used to describe small representative units of a structure's geometry, while *patterns* propagate the tiles into a space-filling structure. These levels are independent and polymorphic, such that a pattern can be applied to any number of tiles, and vice-versa.

Tiles Tiles serve two purposes in MetaDSL: (1) representing structural geometry within some finite, embedded convex polytope (CP), $\Pi_{\text{emb}} \subset \mathbb{R}^3$; and (2) maintaining structured information about their contents, which can be queried to determine validity and/or compatibility. To

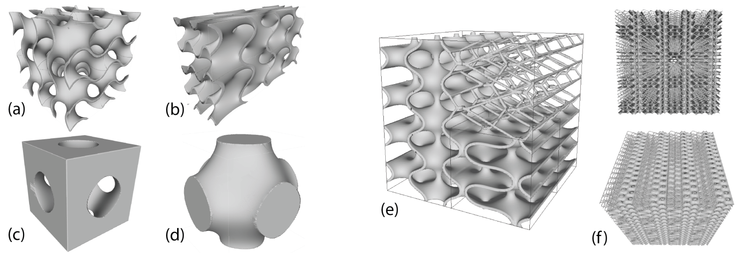

Figure 3: Using a different geometry kernel, MetaDSL captures structures that are impractical or impossible via our default, ProcMeta. **(a-d)** Implicit function-based structures: gyroid sheet TPMS over uniform (a) and non-uniform (b) tiles, and the Schwarz P exo-network (c) and endo-network (d). **(e,f)**: Multi-tile pattern interleaving compatible structures from Figure 1(e) and Figure 2(b,c) to form a larger triply-periodic cell; (e) shows one multi-tile unit, while (f) shows two views of a 4x4x4 block.

facilitate these goals, tile contents are defined using local coordinates relative to Π_{abs}, which is an abstract (non-embedded) CP (e.g., cuboid, tetrahedron) of the same type as Π_{emb}. The MetaDSL snippet `v0=vertex(cuboid.edges.TOP_LEFT, [0.5])` instantiates a vertex of type `PointOnCPEdge` at the midway point of the cuboid edge. Similarly, an edge between `v0` and `v1=vertex(cuboid.faces.TOP)` would return an `EdgeContainedWithinCPFace`. As typed vertices and edges form larger structures such as `skeletons`, their classifications are used to deduce and record broader structural relationships. For example, by querying the skeleton in Figure 1(a), we find that it comprises a single connected component of type `SIMPLE_CLOSED_LOOP`, with 1D incidence on every face of Π_{abs}. This classification is used to judge a skeleton's suitability for a given *lifting function*, which is a procedure used to promote a skeleton into volumetric geometry, or a `LiftedSkeleton` (Figure 1(b)). To complete our Tile (Figure 1(c)), we need only assign a set of corner positions mapping $\Pi_{\text{abs}} \rightarrow \Pi_{\text{emb}} \subseteq \mathbb{R}^3$, then instantiate the relative vertices of the lifted skeleton accordingly. The proposed embedding is validated by Π_{abs} to ensure that it preserves convexity and any angle or length constraints specific to Π_{abs}.

The Tile object is key to MetaDSL's representational power: although many works rely on the *concept* of a tile [Makatura et al., 2023, Panetta et al., 2015, Abu-Mualla and Huang, 2024, Mirramezani et al., 2025], no previous works instantiate tiles as entities against which structural elements can be referenced, analyzed, and queried in the service of verifiable composition (RD5). Our Tiles can be populated with any combination of beams, shells, and other architectural elements (RD1). Moreover, the distinction between Π_{abs} and Π_{emb} improves modularity (RD2) by seamlessly changing tile embeddings (Figure 2(d,e)). Our relative position specifiers also increase semantic meaning and readability (RD3), facilitate robust exploration (RD4), and circumvent the numerical values and computations that often prove challenging for VLMs (RD3, RD4) [Makatura et al., 2024a,b].

Patterns To promote a tile into a space-filling object, MetaDSL applies a *pattern* composed of spatial procedures such as mirrors and rotations. Patterns can only be applied to embedded tiles, because their admissibility is influenced by extrinsic factors such as the dihedral angles of Π_{emb}. However, our pattern operations use lazy evaluation, such that they can be pre-composed over generic Π_{abs}. As before, pattern operations are specified using local coordinates relative to Π_{abs} – e.g. a mirror across `cuboid.faces.TOP`. Through pattern composition, tiles can be propagated according to e.g. periodic tilings given by crystallographic space groups [Adams and Orbanz, 2023], or perhaps even aperiodic tilings from procedural pattern generators. Such complex patterns are possible because the tile's structured data allows us to verify local pattern compatibility based on boundary adjacency.

The combination of a Tile and a Pattern yields a `Structure`, which is a complete representation of the metamaterial. In a final layer, we provide standard constructive solid geometry (CSG) Boolean operations to combine multiple Structures. This makes it easy to define metamaterials with mixed scales, interpenetrating lattices [White et al., 2021], or multi-tile patterns, as shown in Figure 3(e,f).

3.2 Implementation and Extensibility

We implement MetaDSL as an embedded DSL in Python, which provides a familiar, flexible interface with support for comments, descriptive variables, and programmatic constructs such as loops, modules,

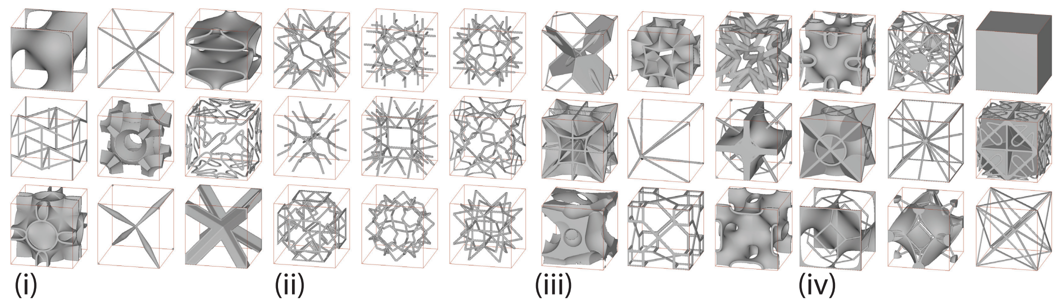

Figure 4: Assortment of metamaterials in MetaDB, illustrating four creation modes: (i) hand-authored seeds, (ii) generated models, (iii) type-enabled mutations, and (iv) LLM-augmented hybrids.

and parameters (RD2, RD3, RD5). For a detailed description of the current language design, implementation, system design insights, and a comparison to ProcMeta, please see Appendix B. The complete MetaDSL documentation is in Appendix G.2.

MetaDSL does not include a geometry kernel, but `Structure` objects can be transpiled to many existing representations. We target the graph format of Procedural Metamaterials (ProcMeta) [Makatura et al., 2023], as their skeletal design space specifically supports a variety of metamaterial classes (RD1). This choice of backend directly influenced MetaDSL's core functionality, as evidenced by MetaDSL's similar initial features (abstract CP types, lifting functions, etc.) and its omissions. For example, MetaDSL currently prioritizes patterns that yield translationally-tileable unit cubes, as ProcMeta only produces geometries in that scope. However, since MetaDSL can be transpiled to any kernel, it is not inherently bound by these limitations. As a proof-of-concept, we built a separate pathway – complete with a basic geometry kernel, a transpilation layer, and new MetaDSL language features – to support structures based on signed distance fields (SDFs). Details are in Appendix B.5. As shown in Figure 3(a-d), this allows MetaDSL to capture myriad structures that are common in metamaterial literature [Fisher et al., 2023], yet impractical or impossible to represent in ProcMeta– including those residing in a non-unit cube. This highlights the flexibility of MetaDSL's design philosophy and its ability to expand without invalidating existing examples.

4 Database Generation

By leveraging MetaDSL, we amass a large, multifaceted metamaterial database (**MetaDB**) containing code, watertight geometry, renderings, and simulated properties for every entry. For quality control, we only add *validated* models that pass basic geometric and physical checks (see Appendix C.6).

4.1 Constructing Metamaterial Models

Each metamaterial is a DSL program, or *model*, that may optionally expose a set of design parameters (with default values). Our metadata block allows program authors to include details such as bounds, dependencies, or recommended ranges for each parameter. This clarifies design freedom, enables continuous exploration, and provides hooks for optimization schemes. The metadata is stored in a machine-parsable format (YAML) with a prepopulated scheme for tracking e.g. provenance, versioning, and notable traits about the structure, including symmetries, architecture type (beams, shells, etc.), and related structures. Our metadata also permits custom fields.

Direct Construction *Authored* models are human-written, with provenance records tracking the model author and the original design source(s), and editable semantic parameters to encode families of models. We also provide a programmatic *generator* interface to create families of models. As a proof of concept, we implemented a generator following Panetta et al. [2015]; this generates parametrized models for all 1,205 truss topologies using a few hundred lines of Python. Our type-checked DSL allows us to specify and evaluate validity constraints on the small tile, without needing to generate the fully-patterned beam network. Moreover, because our generator is exposed and editable, we can easily modify the high-level generator parameters (e.g. maximum vertex valence) to output different sub- or supersets of interest. For each *generated* model, the provenance metadata stores the generator script, its settings, and per-instance parameters; generator parameters may be substituted for specific values or passed through to remain exposed in the resulting programs.

Augmentation We propose two orthogonal protocols to enlarge MetaDB based on existing models. Our first strategy, *Hybridization* (crossover), is motivated by works that offer unique, extremal mechanical properties by hybridizing common structures such as trusses+woven beams [Surjadi et al., 2025], nested trusses [Boda et al., 2025], TPMS shells+planar shells [Chen et al., 2019], and trusses+solids [White et al., 2021]. We emulate this process by prompting an LLM with pairs or triplets of parent programs, then requesting hybrid code. Our prompting strategy (detailed in Appendix C.3) follows insights from recent works in LLM-mediated program search [Li et al., 2025, Romera-Paredes et al., 2024]. The resulting *hybridized* model stores its parent IDs, prompt details, and LLM details as provenance information.

Our second strategy, *mutation*, uses traditional program analysis along with MetaDSL's type system to apply targeted edits – e.g., adjusting skeletal elements or swapping lifting/patterning procedures – as shown in Figure 2. Details are in Appendix C.4. These variations are motivated by works such as Akbari et al. [2022], which posits beam approximations of TPMS shells. Each mutation stores its parent and details about the mutator function.

4.2 Auxiliary Data Generation

For every model we generate three auxiliary artifacts: geometry, renderings, and physical property predictions. To obtain the geometry, we transpile our MetaDSL model into a ProcMeta graph [Makatura et al., 2023] and use their geometry kernel to export a watertight `.obj`. Using the exported mesh, our custom PyRender scene produces orthographic images from the front, top, right, and front-top-right viewpoints. Finally, we use the integrated simulations of ProcMeta to voxelize the mesh on a 100^3 grid and perform periodic homogenisation using a base material with $E{=}1$, $\rho{=}1$, $\nu{=}0.45$. The resulting $6{\times}6$ stiffness matrix C is reduced to 18 scalars: six global metrics—Young's modulus E, shear modulus G, Poisson ratio ν, bulk modulus K, anisotropy A, volume fraction V—plus directional values for E (3), G (3), and ν (6). More details are available in Appendix C.5. MetaDB therefore combines code, geometry, simulation, imagery, and rich provenance—providing a unified benchmark and a data-efficient training ground for vision–language metamaterial assistants.

5 Benchmark Curation

From MetaDB we derive a benchmark that covers three fundamental metamaterial tasks: **(1) reconstruction**—produce a DSL program that reproduces a target structure (for example, from images); **(2) material understanding**—predict the property profile of a given structure description; and **(3) inverse design**—generate a DSL program that satisfies a requested property profile. Each task supports multiple *query types* based on the inputs available. For instance, material understanding may be invoked with a single image ("1-view") or with four images plus code ("multiview_and_code"). The benchmark suite ships a dataset for every query type. We also provide an *omnitask* split that unites every query type into a single corpus; this is useful for training generalist agents.

5.1 Task-Based Dataset Construction

We start with a designated pool of *active* models and partition them into train, validation, and test splits that remain fixed for all tasks. The relevant information for each query type is as follows.

Reconstruction. Given $n \in \{1, \ldots, 4\}$ orthographic images, the desired output is a DSL program whose rendered geometry matches the target. Because every model has four views (Section 4.2), each model contributes $\binom{4}{n}$ examples to the n-view dataset.

Material understanding. Given a structure description, the desired output predicts six global properties: Young's modulus E, shear modulus G, bulk modulus K, Poisson ratio ν, anisotropy A, and volume fraction V. Values are rounded to two significant figures. Our benchmark supports two query types: *multiview_and_code* (four images + DSL code) and *single_image* (one image). The relative performance on each type indicates whether additional context helps or hinders a given VLM.

Table 1: Category-level evaluation results for various models on MetaBench. Valid reports the percentage of valid responses. Average Normalized Error (Error), Chamfer Distance (CD), and Intersection over Union (IoU) are averaged over valid responses across all tasks within a category. SingleTask models average over fewer examples. See Figures 12 to 14 for qualitative evaluation.

Category	Inverse Design		Material Understanding		Reconstruction		
Metric	Error	Valid	Error	Valid	CD	IoU	Valid
Model							
LLaVAOmniTask	**0.011**	**91.9%**	0.024	**100%**	0.034	0.490	82.9%
LLaVASingleTask	0.036	81.9%	**0.018**	**100%**	**0.029**	**0.524**	83.8%
NovaLite	0.060	2.7%	0.200	**100%**	0.119	0.051	19.3%
NovaOmniTask	0.026	91.4%	0.032	**100%**	0.045	0.334	**87.2%**
NovaSingleTask	0.032	79.2%	0.153	**100%**	0.059	0.205	84.8%
OpenAIO3	0.038	24.7%	0.077	**100%**	0.053	0.147	54.6%

Inverse design. Given a target property profile, the desired output is a DSL program whose simulated properties satisfy the profile. We generate datasets for six query types, where the length-n query requests $n \in \{1, \ldots, 6\}$ property targets per profile. Targets may be exact values, ranges, or upper/lower bounds—e.g., "auxetic ($\nu < 0$)" or "volume fraction $V \approx 0.6$." To construct target profiles from a model, we (1) sample n active properties from the model, (2) choose bounds for each, and (3) render a natural-language prompt using a grammar conditioned on each property's part-of-speech tag (adjective, verb, etc.). This process is detailed in Appendix E.2. Both the prompt and the underlying numeric targets are stored, so users can rephrase questions or bypass NLP entirely.

5.2 Task-Based Example Format

The query/response pairs are constructed using task-specific prompt templates (see Appendix G). Given a metamaterial and a task type, we first gather any data used to construct the query/ground truth response or evaluate the predicted response. This is stored in a model-agnostic intermediate format, as detailed in Appendix E.1. Notably, this format allows researchers to reframe prompts without regenerating or deviating from the core content of the inquiry. It also makes MetaBench applicable to traditional non-AI methods. However, since no traditional methods cover the full breadth of MetaBench, we do not include traditional baselines in our evaluations.

6 Results

6.1 Database

MetaDB is, to our knowledge, one of the largest metamaterial databases ever collected, comprising $153,263$ materials. Expert designs comprise 24% (36,997 entries) of the database; this includes 1,588 variations of 50 hand-authored programs, 1,205 generations, and 34,204 generation parameter variations. We also introduce 12,029 hybrids (LLM-generated) and 141,234 mutations (generated via program analysis). To validate MetaDB, we examine its property gamut relative to that of our expert seeds. Both are centered around similar ranges, suggesting that our design space is valid and relevant. However, MetaDB offers more uniform, dense coverage, along with a wider range for properties like anisotropy (~2x the expert range) and directional Poisson ratios (~1.2-4x the expert range).

6.2 Benchmark & Baseline

The 13,282 authored, generated, and hybrid models form the core set from which MetaBench is sampled. We randomly split these models into 500 test, 50 validation, and 12,732 training materials, and generated benchmark tasks for each as described in Section 5. Then, we tested a variety of commercial and open source VLMs on MetaBench, both fine-tuned and zero-shot. Table 1 summarizes these models' performance at the task category level; additional tables and galleries in Appendix D break down performance at the task level, with confidence intervals and qualitative interpretations.

Evaluation Metrics The error metrics for each task are as follows. *Material reconstruction* measures 3D structure similarity, calculated by the intersection over union (IoU) and volumetric chamfer distance of the voxelized unit cells. *Material understanding* measures the Averaged Normalized Error (ANE) across six properties described in Section 5.1, with each normalized based on its typical range within the core material set. Finally, *inverse design* uses a clipped ANE. For properties with specific value targets, the normalized error (NE) is computed as before. For bound targets, NE is taken relative to the bounded region; if the bound is respected, the error is zero.

Models & Implementation We tested 3 base models: a small open-source VLM (LLaVA-Next), a large commercial VLM (Amazon Nova Lite), and a large commercial chain-of-thought reasoning model (Open AI o3 with medium reasoning). We also used the MetaBench training set to produce 4 fine-tuned variants for each of 2 models (LLaVA-Next and Nova Lite). This included one OmniTask model trained over all training examples in MetaBench, and three SingleTask variants trained over one category-representative task type each (4-view reconstruction, 4-target inverse design, and multi-view-plus-code material understanding). Table 1 condenses the SingleTask variants of each model into a single row for compactness. Untuned LLaVA-Next is excluded from the table as it failed to produce any valid output (likely because the MetaDSL description overwhelmed its context window).

LLaVA models are tuned from Llama3-LLaVA-Next-8b [Li et al., 2024, Liu et al., 2024]. Commercial models were tuned and tested with default settings. All tuned models were trained for 1 epoch. For full training and inference details, see Appendix F. Benchmark construction and model prompts are detailed in Appendix E and Appendix G.

Experimental Insights Our experiments revealed three primary insights. First, fine-tuning is necessary for strong performance on MetaBench: untuned reasoning models (o3) can approach weaker tuned models when they manage to produce valid output, but they struggle to do so consistently. Here, responses are invalid if they do not contain the task's requested content (i.e., code, json), or if the generated code fails to produce a valid metamaterial (as defined in Appendix C.6). Our second insight is that fine-tuning generalist multi-task models improves inverse design performance. Finally, a tuned small model outperforms a tuned large model in nearly all metrics. However, this is likely due to it being able to converge more quickly given the same training budget (see Appendix F.1).

6.3 Interactive Case Studies

To explore practical scenarios, we built a browser-based metamaterial copilot interface (Figure 5, left), featuring a VLM chat window, a code editor, and a material preview window. We use NovaLiteOmniTask as the interactive model due to its large context window and strong conversational abilities. We present here two scenarios illustrating the potential of a metamaterial design copilot.

The first scenario creates a material from an input image, as one might do when trying to (re)create naturally-occurring structures, materials pictured in literature, or sketched design concepts. Figure 5 shows this functionality with a material from the MetaBench test set; even with our conversational (rather than structured) request, we were still able to obtain and fabricate a perfect reconstruction.

The second scenario is iterative inverse design (Figure 6), in which we specify a set of target property bounds, and the model generates a metamaterial that satisfies them (as verified with our simulator). But design is always iterative, and seeing one design can spark new criteria and objectives. In this case we wanted a thicker structure that still conformed to our original input; again, the model was able to update the design within target parameters. This illustrates LLMs' powerful ability to remember and carry through *design context*, allowing for assistance across multiple design iterations.

7 Discussion, Limitations, and Future Work

Metamaterial design is a high-impact, multimodal problem that requires complex reasoning and preference consideration, which makes it a natural test bed for AI development. Conversely, metamaterial researchers have called for better data sets and AI-powered tools. MetaDSL and MetaDB provide a common, traceable descriptor that both communities can adopt. As researchers contribute new designs in this format, the database will grow organically, giving machine-learning practitioners richer training data while delivering state-of-the-art design assistants to materials scientists.

Our work provides a comprehensive framework toward these goals, with many avenues for improvement. MetaAssist was deliberately restricted to simple supervised fine tuning to provide a

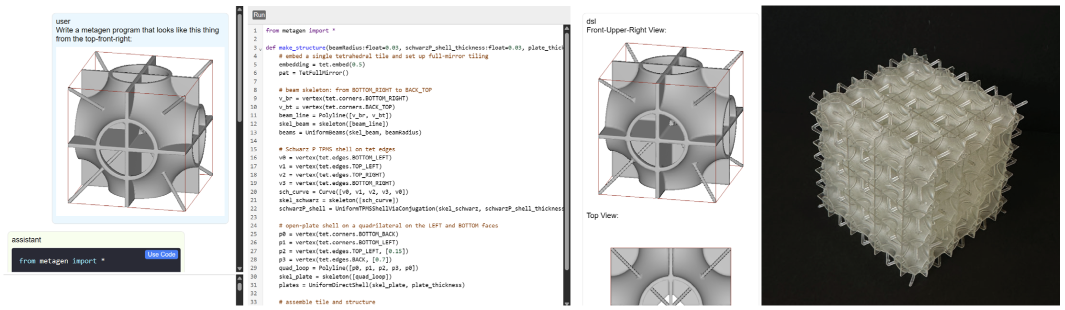

user
Write a metagen program that looks like this thing from the top-front-right:

assistant

```
from metagen import *
```

```
from metagen import *

def make_structure(beamRadius:float=0.03, schwarzP_shell_thickness:float=0.03, plate_thick
    # embed a single tetrahedral tile and set up full-mirror tiling
    embedding = tet.embed(0.5)
    pat = TetFullMirror()

    # beam skeleton: from BOTTOM_RIGHT to BACK_TOP
    v_br = vertex(tet.corners.BOTTOM_RIGHT)
    v_bt = vertex(tet.corners.BACK_TOP)
    beam_line = Polyline([v_br, v_bt])
    skel_beam = skeleton([beam_line])
    beams = UniformBeams(skel_beam, beamRadius)

    # Schwarz P TPMS shell on tet edges
    v0 = vertex(tet.edges.BOTTOM_LEFT)
    v1 = vertex(tet.edges.TOP_LEFT)
    v2 = vertex(tet.edges.TOP_RIGHT)
    v3 = vertex(tet.edges.BOTTOM_RIGHT)
    sch_curve = Curve([v0, v1, v2, v3, v0])
    skel_schwarz = skeleton([sch_curve])
    schwarzP_shell = UniformTPMSShellViaConjugation(skel_schwarz, schwarzP_shell_thickness

    # open-plate shell on a quadrilateral on the LEFT and BOTTOM faces
    p0 = vertex(tet.corners.BOTTOM_BACK)
    p1 = vertex(tet.corners.BOTTOM_LEFT)
    p2 = vertex(tet.edges.TOP_LEFT, [0.15])
    p3 = vertex(tet.edges.BACK, [0.7])
    quad_loop = Polyline([p0, p1, p2, p3, p0])
    skel_plate = skeleton([quad_loop])
    plates = UniformDirectShell(skel_plate, plate_thickness)

    # assemble tile and structure
```

Figure 5: Reconstruction: (Left) Generating a metamaterial program from an input image enables incorporating designs from literature, sketches, and nature. (Right) 3D printed design.

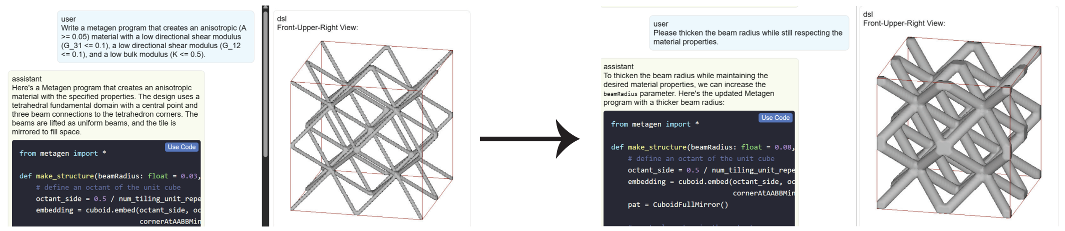

user
Write a metagen program that creates an anisotropic (A >= 0.05) material with a low directional shear modulus (G_31 <= 0.1), a low directional shear modulus (G_12 <= 0.1), and a low bulk modulus (K <= 0.5).

assistant
Here's a Metagen program that creates an anisotropic material with the specified properties. The design uses a tetrahedral fundamental domain with a central point and three beam connections to the tetrahedron corners. The beams are lifted as uniform beams, and the tile is mirrored to fill space.

```
from metagen import *

def make_structure(beamRadius: float = 0.03,
    # define an octant of the unit cube
    octant_side = 0.5 / num_tiling_unit_repe
    embedding = cuboid.embed(octant_side, oc
                             cornerAtAABBMin
```

user
Please thicken the beam radius while still respecting the material properties.

assistant
To thicken the beam radius while maintaining the desired material properties, we can increase the `beamRadius` parameter. Here's the updated Metagen program with a thicker beam radius:

```
from metagen import *

def make_structure(beamRadius: float = 0.08,
    # define an octant of the unit cube
    octant_side = 0.5 / num_tiling_unit_repe
    embedding = cuboid.embed(octant_side, oc
                             cornerAtAABBMin
    pat = CuboidFullMirror()
```

Figure 6: Iterative Inverse Design: Designers can specify desired target properties, and these preferences and constraints can be considered throughout multiple design iterations.

bedrock baseline for our new task. Future works may incorporate RAG to read papers and retrieve patterns, CoT reasoning to connect design intent to property profiles, or RL with curriculum learning to generalize to novel inverse design profiles. Future works may also leverage MetaDSL's retargetability (Appendix A): faster, more flexible kernels would enable larger interactive workflows, simulation-in-the-loop optimization, even-wider dataset scales, and non-cubic and/or aperiodic tilings.

MetaDB also has ample opportunities for growth as a community project, including the implementation of additional generators [Sun et al., 2023a, Liu et al., 2022, Abu-Mualla and Huang, 2024, Makatura et al., 2023], systematic inclusion of singular design templates from metamaterial literature, and diversity-guided synthesis. Our program's explicit semantic structure could support taxonomy construction and intelligent exploration of large design spaces. With broad participation, MetaDB could become the primary resource for tracking metamaterial lineages, structure–property relationships, and mechanistic insights—paralleling the role ImageNet played in computer vision.

As our framework grows, we will also need safety guardrails to mitigate the potential for errors or misguided application. This deserves particular attention in a domain like metamaterials, which is complex and rapidly evolving, yet targeting applications in which failures may be catastrophic. As such, results must be validated and communication measured. Our format already takes small strides toward transparency by maintaining detailed provenance records, and releasing our artifacts along with the pipelines used to generate them. Moving forward, it would be prudent to include additional safeguards such as automated validity checks, uncertainty estimates, and safety factors.

8 Conclusion

We introduced **MetaGen**, a unified ecosystem for vision–language metamaterial design that combines (i) *MetaDSL*, a compact yet expressive domain-specific language; (ii) *MetaDB*, a 150 000-entry database with paired geometry, renderings, and physics; (iii) *MetaBench*, a task-oriented benchmark that probes reconstruction, material understanding, and inverse design; and (iv) *MetaAssist*, the first VLM-driven CAD interface for architected materials. Our baseline experiments illustrate that VLMs offer promising performance for multi-modal translation and design generation. Moreover, we provide a holistic vision for accelerated, symbiotic research at the intersection of machine learning and architected materials. With MetaGen as both a challenging benchmark for VLMs and a practical toolkit for materials scientists, our paper lays the foundation to bring this vision to life.

Acknowledgments and Disclosure of Funding

The authors acknowledge the generous financial support of Amazon AGI-C, through an ongoing MIT Science Hub grant. The authors also express their sincere gratitude to the Amazon AGI-C team, who have provided immeasurable support throughout this project, ranging from high-level discussions to detailed technical support regarding the Nova models and surrounding infrastructure. Finally, the authors would like to thank Beichen Li for providing the code for VLMaterial, on which an early version of our data-generation and ML training pipelines were based.

References

Benjamin Jenett, Christopher Cameron, Filippos Tourlomousis, Alfonso Parra Rubio, Megan Ochalek, and Neil Gershenfeld. Discretely assembled mechanical metamaterials. *Science Advances*, 6(47), 2020.

Sahab Babaee, Jongmin Shim, James C Weaver, Elizabeth R Chen, Nikita Patel, and Katia Bertoldi. 3d soft metamaterials with negative poisson's ratio. *Advanced Materials*, 25(36), 2013.

Zhao Qin, Gang Seob Jung, Min Jeong Kang, and Markus J. Buehler. The mechanics and design of a lightweight three-dimensional graphene assembly. *Science Advances*, 3(1), 2017.

James Utama Surjadi, Bastien F G Aymon, Molly Carton, and Carlos M Portela. Double-network-inspired mechanical metamaterials. *Nat Mater*, April 2025.

Zhaohui Fan, Renjing Gao, and Shutian Liu. Thermal conductivity enhancement and thermal saturation elimination designs of battery thermal management system for phase change materials based on triply periodic minimal surface. *Energy*, 259, 2022.

Reza Attarzadeh, Seyed-Hosein Attarzadeh-Niaki, and Christophe Duwig. Multi-objective optimization of tpms-based heat exchangers for low-temperature waste heat recovery. *Applied Thermal Engineering*, 212, 2022.

Arash Ataee, Yuncang Li, Darren Fraser, Guangsheng Song, and Cuie Wen. Anisotropic ti-6al-4v gyroid scaffolds manufactured by electron beam melting (ebm) for bone implant applications. *Materials & Design*, 137, 2018.

Rita Ambu and Anna Eva Morabito. Modeling, assessment, and design of porous cells based on schwartz primitive surface for bone scaffolds. *The Scientific World Journal*, 2019, 2019.

Liane Makatura, Bohan Wang, Yi-Lu Chen, Bolei Deng, Chris Wojtan, Bernd Bickel, and Wojciech Matusik. Procedural metamaterials: A unified procedural graph for metamaterial design. *ACM Trans. Graph.*, 42(5), July 2023. ISSN 0730-0301. doi: 10.1145/3605389.

Doksoo Lee, Wei (Wayne) Chen, Liwei Wang, Yu-Chin Chan, and Wei Chen. Data-driven design for metamaterials and multiscale systems: A review. *Advanced Materials*, 36(8):2305254, 2024. doi: https://doi.org/10.1002/adma.202305254. URL `https://advanced.onlinelibrary.wiley.com/doi/abs/10.1002/adma.202305254`.

Tianyang Xue, Haochen Li, Longdu Liu, Paul Henderson, Pengbin Tang, Lin Lu, Jikai Liu, Haisen Zhao, Hao Peng, and Bernd Bickel. Mind: Microstructure inverse design with generative hybrid neural representation, 2025. URL `https://arxiv.org/abs/2502.02607`.

James Utama Surjadi and Carlos M. Portela. Enabling three-dimensional architected materials across length scales and timescales. *Nature Materials*, 24(4):493–505, Apr 2025. ISSN 1476-4660. doi: 10.1038/s41563-025-02119-8. URL `https://doi.org/10.1038/s41563-025-02119-8`.

Muhammad and C. W. Lim. Phononic metastructures with ultrawide low frequency three-dimensional bandgaps as broadband low frequency filter. *Scientific Reports*, 11(1), 2021.

Tobias Frenzel, Muamer Kadic, and Martin Wegener. Three-dimensional mechanical metamaterials with a twist. *Science*, 358(6366):1072–1074, 2017. doi: 10.1126/science.aao4640. URL `https://www.science.org/doi/abs/10.1126/science.aao4640`.

Timon Meier, Vasileios Korakis, Brian W. Blankenship, Haotian Lu, Eudokia Kyriakou, Savvas Papamakarios, Zacharias Vangelatos, M. Erden Yildizdag, Gordon Zyla, Xiaoxing Xia, Xiaoyu Zheng, Yoonsoo Rho, Maria Farsari, and Costas P. Grigoropoulos. Scalable phononic metamaterials: Tunable bandgap design and multi-scale experimental validation. *Materials & Design*, 252:113778, 2025. ISSN 0264-1275. doi: https://doi.org/10.1016/j.matdes.2025.113778. URL `https://www.sciencedirect.com/science/article/pii/S0264127525001984`.

Julian Panetta, Qingnan Zhou, Luigi Malomo, Nico Pietroni, Paolo Cignoni, and Denis Zorin. Elastic textures for additive fabrication. *ACM Trans. Graph.*, 34(4), July 2015. ISSN 0730-0301. doi: 10.1145/2766937.

Mohammad Abu-Mualla and Jida Huang. A dataset generation framework for symmetry-induced mechanical metamaterials. *Journal of Mechanical Design*, 147(4):041705, 12 2024. ISSN 1050-0472. doi: 10.1115/1.4066169.

Bingteng Sun, Xin Yan, Peiqing Liu, Yang Xia, and Lin Lu. Parametric plate lattices: Modeling and optimization of plate lattices with superior mechanical properties. *Additive Manufacturing*, 72:103626, 2023a. ISSN 2214-8604. doi: https://doi.org/10.1016/j.addma.2023.103626.

Yonglai Xu, Hao Pan, Ruonan Wang, Qiang Du, and Lin Lu. New families of triply periodic minimal surface-like shell lattices. *Additive Manufacturing*, 77:103779, 2023. ISSN 2214-8604. doi: https://doi.org/10.1016/j.addma.2023.103779.

Peiqing Liu, Bingteng Sun, Jikai Liu, and Lin Lu. Parametric shell lattice with tailored mechanical properties. *Additive Manufacturing*, 60:103258, 2022. ISSN 2214-8604. doi: https://doi.org/10.1016/j.addma.2022.103258.

Zhenze Yang and Markus J. Buehler. High-throughput generation of 3d graphene metamaterials and property quantification using machine learning. *Small Methods*, 6(9):2200537, 2022. doi: https://doi.org/10.1002/smtd.202200537.

Yu-Chin Chan, Faez Ahmed, Liwei Wang, and Wei Chen. METASET: Exploring Shape and Property Spaces for Data-Driven Metamaterials Design. *Journal of Mechanical Design*, 143(3), 2020.

J. B. Berger, H. N. G. Wadley, and R. M. McMeeking. Mechanical metamaterials at the theoretical limit of isotropic elastic stiffness. *Nature*, 543(7646):533–537, Mar 2017. ISSN 1476-4687. doi: 10.1038/nature21075. URL `https://doi.org/10.1038/nature21075`.

Zeyao Chen, Yi Min Xie, Xian Wu, Zhe Wang, Qing Li, and Shiwei Zhou. On hybrid cellular materials based on triply periodic minimal surfaces with extreme mechanical properties. *Materials & Design*, 183:108109, 2019. ISSN 0264-1275. doi: https://doi.org/10.1016/j.matdes.2019.108109. URL `https://www.sciencedirect.com/science/article/pii/S0264127519305477`.

Benjamin C. White, Anthony Garland, Ryan Alberdi, and Brad L. Boyce. Interpenetrating lattices with enhanced mechanical functionality. *Additive Manufacturing*, 38:101741, 2021. ISSN 2214-8604. doi: https://doi.org/10.1016/j.addma.2020.101741. URL `https://www.sciencedirect.com/science/article/pii/S2214860420311131`.

Yanyan Yang, Lili Wang, Xiaoya Zhai, Kai Chen, Wenming Wu, Yunkai Zhao, Ligang Liu, and Xiao-Ming Fu. Guided diffusion for fast inverse design of density-based mechanical metamaterials, 2024a. URL `https://arxiv.org/abs/2401.13570`.

Beichen Li, Rundi Wu, Armando Solar-Lezama, Liang Shi, Changxi Zheng, Bernd Bickel, and Wojciech Matusik. VLMaterial: Procedural material generation with large vision-language models. In *The Thirteenth International Conference on Learning Representations*, 2025. URL `https://openreview.net/forum?id=wHebuIb6IH`.

Yue Yang, Fan-Yun Sun, Luca Weihs, Eli VanderBilt, Alvaro Herrasti, Winson Han, Jiajun Wu, Nick Haber, Ranjay Krishna, Lingjie Liu, et al. Holodeck: Language guided generation of 3d embodied ai environments. In *Proceedings of the IEEE/CVF Conference on Computer Vision and Pattern Recognition*, pages 16227–16237, 2024b.

Vikram Kumaran, Jonathan Rowe, Bradford Mott, and James Lester. Scenecraft: automating interactive narrative scene generation in digital games with large language models. In *Proceedings of the AAAI Conference on Artificial Intelligence and Interactive Digital Entertainment*, volume 19, pages 86–96, 2023.

Chunyi Sun, Junlin Han, Weijian Deng, Xinlong Wang, Zishan Qin, and Stephen Gould. 3d-gpt: Procedural 3d modeling with large language models. *arXiv preprint arXiv:2310.12945*, 2023b.

Zhengyi Wang, Jonathan Lorraine, Yikai Wang, Hang Su, Jun Zhu, Sanja Fidler, and Xiaohui Zeng. Llama-mesh: Unifying 3d mesh generation with language models. *arXiv preprint arXiv:2411.09595*, 2024.

R Kenny Jones, Paul Guerrero, Niloy J Mitra, and Daniel Ritchie. Shapelib: designing a library of procedural 3d shape abstractions with large language models. *arXiv preprint arXiv:2502.08884*, 2025.

Ian Huang, Guandao Yang, and Leonidas Guibas. Blenderalchemy: Editing 3d graphics with vision-language models. In *European Conference on Computer Vision*, pages 297–314. Springer, 2024.

Yutaro Yamada, Khyathi Chandu, Yuchen Lin, Jack Hessel, Ilker Yildirim, and Yejin Choi. L3go: Language agents with chain-of-3d-thoughts for generating unconventional objects. *arXiv preprint arXiv:2402.09052*, 2024.

Ata Çelen, Guo Han, Konrad Schindler, Luc Van Gool, Iro Armeni, Anton Obukhov, and Xi Wang. I-design: Personalized llm interior designer, 2024.

Kiyohiro Nakayama, Jan Ackermann, Timur Levent Kesdogan, Yang Zheng, Maria Korosteleva, Olga Sorkine-Hornung, Leonidas Guibas, Guandao Yang, and Gordon Wetzstein. Aipparel: A large multimodal generative model for digital garments. *Computer Vision and Pattern Recognition (CVPR)*, 2025.

Siyuan Bian, Chenghao Xu, Yuliang Xiu, Artur Grigorev, Zhen Liu, Cewu Lu, Michael J Black, and Yao Feng. Chatgarment: Garment estimation, generation and editing via large language models. 2025.

Liane Makatura, Michael Foshey, Bohan Wang, Felix Hähnlein, Pingchuan Ma, Bolei Deng, Megan Tjandrasuwita, Andrew Spielberg, Crystal Owens, Peter Yichen Chen, Allan Zhao, Amy Zhu, Wil Norton, Edward Gu, Joshua Jacob, Yifei Li, Adriana Schulz, and Wojciech Matusik. How Can Large Language Models Help Humans in Design and Manufacturing? Part 1: Elements of the LLM-Enabled Computational Design and Manufacturing Pipeline. *Harvard Data Science Review*, (Special Issue 5), dec 23 2024a. https://hdsr.mitpress.mit.edu/pub/15nqmdzl.

Liane Makatura, Michael Foshey, Bohan Wang, Felix Hähnlein, Pingchuan Ma, Bolei Deng, Megan Tjandrasuwita, Andrew Spielberg, Crystal Owens, Peter Yichen Chen, Allan Zhao, Amy Zhu, Wil Norton, Edward Gu, Joshua Jacob, Yifei Li, Adriana Schulz, and Wojciech Matusik. How Can Large Language Models Help Humans in Design And Manufacturing? Part 2: Synthesizing an End-to-End LLM-Enabled Design and Manufacturing Workflow. *Harvard Data Science Review*, (Special Issue 5), dec 23 2024b. https://hdsr.mitpress.mit.edu/pub/hiii8fyn.

Jiin Choi, Seung Won Lee, and Kyung Hoon Hyun. Genpara: Enhancing the 3d design editing process by inferring users' regions of interest with text-conditional shape parameters. In *Proceedings of the 2025 CHI Conference on Human Factors in Computing Systems*, CHI '25, New York, NY, USA, 2025. Association for Computing Machinery. ISBN 9798400713941. doi: 10.1145/3706598.3713502. URL `https://doi.org/10.1145/3706598.3713502`.

Haocheng Yuan, Jing Xu, Hao Pan, Adrien Bousseau, Niloy J. Mitra, and Changjian Li. Cadtalk: An algorithm and benchmark for semantic commenting of cad programs. In *2024 IEEE/CVF Conference on Computer Vision and Pattern Recognition (CVPR)*, pages 3753–3762, 2024. doi: 10.1109/CVPR52733.2024.00360.

Feng Zhou, Ruiyang Liu, Chen Liu, Gaofeng He, Yong-Lu Li, Xiaogang Jin, and Huamin Wang. Design2garmentcode: Turning design concepts to tangible garments through program synthesis. 2025.

Mehran Mirramezani, Anne S. Meeussen, Katia Bertoldi, Peter Orbanz, and Ryan P Adams. Designing mechanical meta-materials by learning equivariant flows. In *The Thirteenth International Conference on Learning Representations*, 2025. URL `https://openreview.net/forum?id=VMurwgAFWP`.

Ryan P. Adams and Peter Orbanz. Representing and learning functions invariant under crystallographic groups, 2023. URL `https://arxiv.org/abs/2306.05261`.

Joseph W. Fisher, Simon W. Miller, Joseph Bartolai, Timothy W. Simpson, and Michael A. Yukish. Catalog of triply periodic minimal surfaces, equation-based lattice structures, and their homogenized property data. *Data in Brief*, 49:109311, 2023. ISSN 2352-3409. doi: https://doi.org/10.1016/j.dib.2023.109311. URL `https://www.sciencedirect.com/science/article/pii/S2352340923004298`.

Ramalingaiah Boda, Biranchi Panda, and Shanmugam Kumar. Bioinspired design of isotropic lattices with tunable and controllable anisotropy. *Advanced Engineering Materials*, 27(11):2401881, 2025. doi: https://doi.org/10.1002/adem.202401881. URL `https://advanced.onlinelibrary.wiley.com/doi/abs/10.1002/adem.202401881`.

Bernardino Romera-Paredes, Mohammadamin Barekatain, Alexander Novikov, Matej Balog, M. Pawan Kumar, Emilien Dupont, Francisco J. R. Ruiz, Jordan S. Ellenberg, Pengming Wang, Omar Fawzi, Pushmeet Kohli, and Alhussein Fawzi. Mathematical discoveries from program search with large language models. *Nature*, 625(7995):468–475, Jan 2024. ISSN 1476-4687. doi: 10.1038/s41586-023-06924-6. URL `https://doi.org/10.1038/s41586-023-06924-6`.

Mostafa Akbari, Armin Mirabolghasemi, Mohammad Bolhassani, Abdolhamid Akbarzadeh, and Masoud Akbarzadeh. Strut-based cellular to shellular funicular materials. *Advanced Functional Materials*, 32(14): 2109725, 2022. doi: https://doi.org/10.1002/adfm.202109725. URL `https://advanced.onlinelibrary.wiley.com/doi/abs/10.1002/adfm.202109725`.

Feng Li, Renrui Zhang, Hao Zhang, Yuanhan Zhang, Bo Li, Wei Li, Zejun Ma, and Chunyuan Li. Llava-next-interleave: Tackling multi-image, video, and 3d in large multimodal models. *arXiv preprint arXiv:2407.07895*, 2024.

Haotian Liu, Chunyuan Li, Yuheng Li, Bo Li, Yuanhan Zhang, Sheng Shen, and Yong Jae Lee. Llava-next: Improved reasoning, ocr, and world knowledge, January 2024. URL `https://llava-vl.github.io/blog/2024-01-30-llava-next/`.

Edward J Hu, Yelong Shen, Phillip Wallis, Zeyuan Allen-Zhu, Yuanzhi Li, Shean Wang, Lu Wang, Weizhu Chen, et al. Lora: Low-rank adaptation of large language models. *ICLR*, 1(2):3, 2022.

Ilya Loshchilov and Frank Hutter. Decoupled weight decay regularization. *arXiv preprint arXiv:1711.05101*, 2017.

A Ecosystem Design

The four components of the MetaGen ecosystem work together to achieve our design goals. We outline these goals and the design and organization decisions that achieve them here:

- MetaDB
  - Design Goals: Collect existing knowledge in a reconfigurable, reusable, and task independent manner
  - Organization
    - Primary Elements: Material Definitions; Provenance
    - Derived Elements: Geometry; Computed Properties
- MetaBench
  - Design Goals:
  - Organization:
    - Primary Elements: Structured Task Definitions; Target Data; References, Evaluation Procedures
    - Derived Elements: Query Strings; Example Responses
- MetaDSL
  - Design Goals: Eventual Comprehensiveness via Extensibility; Supports Hybrid Structures Easily; Ease of Use
  - Design Decisions: Extensible Embedded Python DSL for extensibility and Ease-of-Us; Separation of Front-End Language from Geometry Kernel
- MetaAssist
  - Design Goals: Usable for general engineers; single interface across design silos; possibility of integrating unstructured data (literature, sketches, etc.)
  - Elements: Interactive Interface; Trained Baseline Models

Each component supports the others, as illustrated in Figure 7

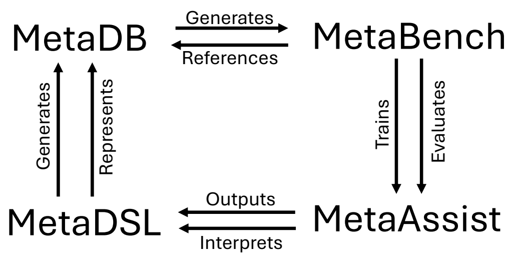

Figure 7: Relationships between MetaGen ecosystem components.

A.1 Ecosystem Development and Insights

The elements of this ecosystem were developed in concert with one another, going through 3 major iterations before arriving at their current state. MetaDSL was at the heart of each iteration, as the representation has a direct impact on the efficacy of the other three components:

- MetaDB needs a representation that captures diverse structures, but also offers robust pathways for scalable (and, in this case, VLM-driven) structure generation, hybridization, mutation, sampling, etc.
- MetaBench can only be used for training and evaluation if it is built atop a large, diverse database.
- MetaAssist relies on a strong training corpus from MetaBench. MetaAssist also hinges on the intelligibility of the representation, and the model's ability to interpret, generate, and modify programs according to user input.

We defer the language-specific development details to Appendix B.6.

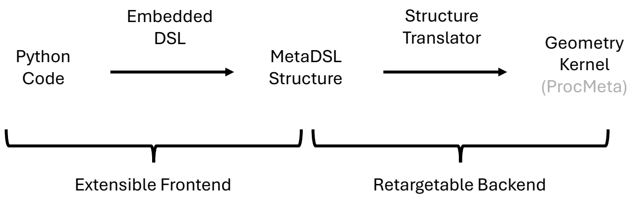

Figure 8: Overview of MetaDSL's implementation. MetaDSL programs are written in an embedded Python DSL frontend to allow for ease of use and extensibility. These structures are compiled into a structured intermediate representation, and a backend Translator converts these structures into geometry kernel instructions. In our implementation we used the geometry kernel from ProcMeta Makatura et al. [2023]. By separating the front-end representation from the backend geometry kernel, MetaDSL is flexible to both be extended in its frontend representation, and retargettable to different geometry backends for new applications, while keeping a compatible material representation.

Outside the scope of the DSL, we also found that dataset management and curation posed a major hurdle. We improved diversity by continuously mining metamaterial literature for additional seed program designs. We expressed these seed programs as-parametrically-as-possible to allow for expert-driven sampling. As we scaled the dataset, we also realized that it would be critical to keep track of the programs' sources and relationship to one another. This information is especially useful for navigation, contextualization and diversity management, particularly as the database grows in response to community effort. To manage this, we introduced a formalized provenance system for MetaDB.

B MetaDSL

B.1 Additional Implementation Details

We implemented the core functionality of MetaDSL (version 1.1.0) with two goals in mind. First, we wanted full support for the metamaterials that were expressible in our geometry kernel, ProcMeta. Second, we wanted our infrastructure to easily permit extensions in the future without invalidating existing programs. We detail the current state of each feature category in our language: convex polytopes, skeletons, lifting procedures, tiles, and patterns. For a full API description of the accessible functions, please refer to Appendix G.2. Figure 8 shows an overview of the compiler architecture.

Convex Polytopes (CP) Currently, all of our programs make use of three pre-defined CPs (as inspired by ProcMeta): `cuboid`, `triPrism` and `tet`. The infrastructure to define custom convex polytopes exists, and most operators up to and including Tiles should generalize to such CPs. However, the patterning operations would need to be generalized before being able to operate on arbitrary CPs.

Skeletons Then, a *skeleton* is constructed via a set of vertices and edges that are positioned relative to a common CP. Each vertex is positioned on a particular CP entity (corner, edge, face, interior). Each CP entity is accessed via a semantically meaningful alias, permitting calls such as e.g. `vertex(cuboid.edges.BACK_LEFT)`. The `vertex` call also optionally takes a list $\vec{t}$ of interpolation values used to position the vertex within the entity. If $\vec{t}$ is omitted, the returned point will be at the entity's midpoint (edge) or centroid (face/interior). Presently, corners ignore weights (since they cannot be moved); edges use linear interpolation; and faces use barycentric coordinates if they contain 3 vertices or bilinear interpolation for quads. If a CP with different polygonal faces (e.g. pentagons) were implemented, an appropriate lower-dimensional vertex positioning specification would need to be devised. Internally, the vertices are stored using weights over a full list of the CP corners, so additional specification interfaces can easily be defined.

An ordered list of vertices can then be strung together into simple (non-branching, self-intersection-free) open or closed paths via the `Polyline` or `Curve` commands. Each edge contained in a path infers and maintains information about its incidence on the CP – including whether it is contained within a face, through the CP volume, coincident with a CP edge, etc. This is very useful when determining lifting function compatibility, as some procedures can only be applied when e.g. every path edge is contained within a CP face.

Then, a `skeleton` is used to combine a set of vertices or polylines/curves into a larger, more complex element, over which additional organizational information is computed. Skeletons infer the connected components formed by the inputs, then categorize them based on their topology. Thus, a skeleton may be labeled as a simple closed loop, even if the input is a set of open paths. Again, these insights are critical for determining the skeleton's compatibility with downstream operations, such as lifting procedures. We also included infrastructure for the skeletons to infer and track their total incidence on each entity of the reference CP, including the dimensionality (e.g. point or line) of an intersection – however, this feature is not fully implemented in the current MetaDSL version.

Lifting Procedures *Lifting procedures* are used to transform the skeleton into a volumetric object. Simple procedures like `Spheres` instantiate a sphere of the given radius centered at each vertex in the skeleton. Similarly, `UniformBeams` instantiates a beam of the given thickness centered along each path of the input skeleton. The shell operators (`UniformDirectShell`, `UniformTPMSShellViaMixedMinimal`, and `UniformTPMSShellViaConjugation`) solve for a surface that spans the provided boundary curve before expanding the surface to the desired thickness. Our shell and beam procedures mimic those defined by ProcMeta, as they cover a wide range of metamaterial classes and were already (by construction) natively supported by our geometry kernel. Our `Curve` and `Polyline` commands correspond to their smooth/non-smooth edge chains, respectively. Unlike the original, we chose to explicitly separate several operators that were previously lumped together, which clarified and minimized the number of exposed parameters for each call.

Tiles To create an embedded, patternable tile, we provide a list of one or more lifted skeletons as input to the `Tile` operator. The tile operator also takes as input the embedding information, which will be used to embed the CP and, in turn, each vertex of the contained skeleton(s). To obtain the embedding information, each CP implements at least one `embed` function, which takes high level parameters such as the min/max position of the CP's AABB.

Because of constraints imposed by $ProcMeta$ – that these must form a partition of the unit cell – our code currently treats these CPs with some additional assumptions. Specifically, though the cuboid need not be a cube, it must have right angles everywhere, and edge lengths must be $1/2^k$ for some positive integer k; in practice, $k \in [1, ..4]$. The triPrism is assumed to be an isoceles triangle with a right angle. The tet similarly has a base that is an isoceles triangle with a right angle, and a fourth vertex that is located directly above one of the 45 degree angles. These assumptions would ideally be relaxed in a future version of MetaDSL.

Patterns Patterns are currently the most restricted feature of MetaDSL, as we restrict our dataset to programs that can be compiled down to the language and solver set described by ProcMeta. Thus, rather than extending our structures to a more arbitrary tiling in $\mathbb{R}^3$, all of our structures have a translational unit residing in a unit cube. The pattern operators were written in a way that allows for additional, extended tiling procedures. We prioritized mirrors, because they are sufficient to express a wide range of common metamaterial designs, and they are often used in generative metamaterial design schemes, as the connectivity requirements are simpler than most other operations. We also have limited support for other operations such as `Rotate180` and `Translate`, which can be used inside the `Custom` pattern specifier. Currently, these limited operations are only defined for specific transformations on cuboids. We look forward to an expanded MetaDSL that includes full support for these patterning operations, at least over the pre-built CPs that currently exist. In the long term, we envision a patterning system that extends well beyond this, to support large, potentially aperiodic or asymmetric tilings composed of one or more tiles with arbitrary CPs. This is a very difficult problem, and will itself present an interesting set of research directions, including how to intuitively specify these patterns and how to characterize their compatibility/validity.

B.2 Example Programs

Example program-structure pairs are listed in Figure 9 and Figure 10. Many additional models can be found in the accompanying data.

B.3 Uniqueness

MetaDSL programs are not naturally unique; there exist many ways to represent a given metamaterial structure. For example: the Schwarz P shown in Figure 9 is represented over a tetrahedral bounding volume representing $1/48$ of structure's the translational unit, but it could just as easily be conceived over a cuboid bounding volume representing $1/8$ of the translational unit, as shown in Figure 1 of Makatura et al. [2023]. There is no clear "best" representation for metamaterials. We could select a minimal representation as the conventional descriptor, which would prioritize the tet-based Schwarz P over the cuboid-based one. However, it may be that the cuboid-based structure is more intuitive for people; since readability is a key consideration in human-facing interfaces, this ought to be considered when selecting standards.

Uniqueness is also difficult because there are often disparate representations that can lead to similar or identical structures. For example, when TPMS structures like the SchwarzP appear in literature, they are most commonly approximated using a simple trigonometric implicit function. We discuss an extended MetaDSL that can

```
from metagen import *

def make_structure( shell_thickness =0.03) -> Structure :
    v0 = vertex ( tet .edges.BOTTOM_LEFT)
    v1 = vertex ( tet .edges.TOP_LEFT)
    v2 = vertex ( tet .edges.TOP_RIGHT)
    v3 = vertex ( tet .edges.BOTTOM_RIGHT)

    c0 = Curve([v0, v1, v2, v3, v0])

    skel = skeleton ([c0])
    shell = UniformTPMSShellViaConjugation(skel, shell_thickness )

    embedding = tet .embed(0.5)
    tile = Tile ([ shell ], embedding)
    pat = TetFullMirror ()
    obj = Structure ( tile , pat )

    return obj
```

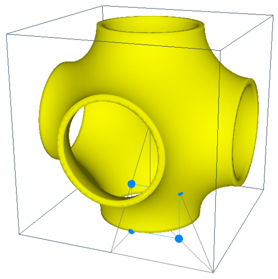

Figure 9: Example program and corresponding geometry for the Schwarz P structure.

```
from metagen import *

def make_structure(beamRadius_narrow=0.03, beamRadius_wide=0.1) -> Structure:
    embed = cuboid.embed(0.5, 0.5, 0.5,
                         cornerAtAABBMin=cuboid.corners.FRONT_BOTTOM_LEFT)

    v0 = vertex (cuboid. corners .FRONT_BOTTOM_LEFT)
    v1 = vertex (cuboid. corners .BACK_TOP_RIGHT)
    p0 = Polyline ([ v0, v1 ])

    skel = skeleton ([ p0])
    liftedSkel = SpatiallyVaryingBeams( skel , [[0, beamRadius_narrow],
                                               [0.5, beamRadius_wide],
                                               [1, beamRadius_narrow]])

    tile = Tile ([ liftedSkel ], embed)
    pat = Custom(Rotate180([cuboid.edges.BACK_RIGHT,
                            cuboid.edges.BACK_LEFT], True,
                 Rotate180([cuboid.edges.TOP_RIGHT], True)))
    obj = Structure ( tile , pat )

    return obj
```

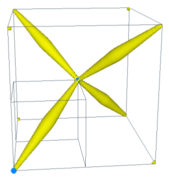

Figure 10: Example program and corresponding geometry for the pentamode structure.

accommodate such implicit functions in Appendix B.5. These are not identical to our ProcMeta-inspired representation above, but they have considerable agreement, and are often considered equivalent in practice.

Moreover, since metamaterials are generally intended to tile $\mathbb{R}^3$, uniqueness can only be determined on the already-tiled scale. This is because there are infinitely many translational unit cubes that lead to the same tiled structure in R^3: the unit cell extracted from $[0]^3 - [1]^3$ is equally valid as the one from $[-0.5]^3 - [0.5]^3$, but they are likely to appear very different on their own.

Because of the ambiguities discussed above, MetaDSL makes no effort to encourage or enforce a canonical representation.* However, our provenance block can be fruitfully used to track relationships such as these – in many of the hand-authored examples, there is already a partial record of related structures that appear in the database. As MetaDSL and MetaDB evolve over time, it would be very interesting to track related representations and establish canonical norms.

$*$ Although MetaDSL currently ignores uniqueness metrics, we do make some preliminary efforts to prevent excessive duplication in MetaDB. Specifically, we evaluate the voxelized representation of our non-expert materials (e.g., hybridizations, augmentations) and compare it to existing samples in the database. The new material candidate is only added if it is sufficiently different.

B.4 MetaDSL vs. ProcMeta

As suggested by Appendix A.1 and the architecture diagram in Figure 8, MetaDSL is distinct from and strictly more general than ProcMeta, with a design philosophy all its own. Our approach was motivated by our early experiments with ProcMeta, which revealed a critical shortcoming: important information was represented implicitly in the ProcMeta GUI interface, and was entirely absent from the ProcMeta graph representation. To make this information accessible to LLMs (and more easily accessible to humans), we implemented a programmatic interface, MetaDSL, that compiles to the same geometry kernel as ProcMeta, but provides several practical advantages (see Table 2).

Most importantly, MetaDSL introduces explicit, referenceable bounding volumes (BVs), which are critical for verifying and enforcing the preconditions of geometry operations. In the ProcMeta GUI, BVs exist only as non-referenceable visual aids; users must manually align coordinates, and no automated compatibility checks are possible. ProcMeta graphs omit BVs entirely. MetaDSL represents BVs through a CP abstraction, which enforces constraints by construction, enables type checking, and cleanly separates tile content from patterning, improving modularity and reconfigurability. These features align the representation more closely with the valid shape space, aiding both human designers and LLMs in producing valid, diverse structures. MetaDSL programs also make heavy use of programmatic features absent from ProcMeta graphs. Semantic variable names, comments (avg. 4/program), and parametric variables improve human interpretability and support natural-language reasoning for LLMs. Loops and helper functions are also common, appearing in 1,744 and 2,103 of the 13,284 core programs respectively. These features allow compact, self-consistent definitions that would be unwieldy if unrolled or inlined into a ProcMeta graph.

We tested LLM-based augmentation using ProcMeta JSON instead of MetaDSL. MetaDSL yielded: (1) higher code validity (75% vs. 54%), (2) more structurally focused reasoning rather than boilerplate handling, and (3) lower token usage (580 vs. 1,049 tokens on average for o4). Beyond these immediate benefits for LLM usage and dataset generation, our DSL interface also makes MetaDSL a more flexible platform from which to build further extensions, which facilitates its intended purpose as the seed of a wider community project.

B.5 Extensibility

The MetaDSL interface naturally generalizes to shape spaces that would be difficult to represent in ProcMeta's graph approach. For example, implicit functions are common in metamaterial design, but they would be cumbersome to represent in ProcMeta's graph. To show that MetaDSL could extend to such structures, we implement a separate, proof-of-concept pipeline that circumvents the ProcMeta backend.

MetaDSL Extension First, we extend the MetaDSL language to accomodate implicit function-based skeleton generators and SDF-based lifting functions. To do this, we introduced a `CartesianVolume` object, which anchors a Cartesian grid to the entities of Π_{abs}, such that local Cartesian coordinates can automatically be transformed into CP-referenced entities. This allows users to define and manipulate SDFs in a familiar workflow, while preserving MetaDSL's abstraction and validation capabilities. An example program is available in Figure 11.

Alternate Geometry Kernel & Transpiler We implemented a simple backend that iteratively builds up a triangle mesh based on the operations (e.g., create vertex, create face, mirror) requested by a topologically-sorted input graph. Our kernel only supports inputs derived from MetaDSL Structures with fully-known geometry at the time of export. This excludes most structures that are derived from ProcMeta-inspired lifting functions (e.g.,

```
from metagen import *
from sdf import *
from tpms_helpers import *
from common_tpms import gyroid

def make_structure(isoval_min: float =-0.2, isoval_max: float =0.2, l: float =1.0)
    -> Structure :

    cv = CartesianVolume(   cuboid.corners.FRONT_BOTTOM_RIGHT,
                            cuboid.corners.FRONT_BOTTOM_LEFT, 1,
                            cuboid.corners.FRONT_TOP_RIGHT,   1,
                            cuboid.corners.BACK_BOTTOM_RIGHT, 1)

    shell_sdf = sheet_isosurface_pair (gyroid, isoval_min, isoval_max)
    shell = cv.liftedSkelsFromSDF( shell_sdf )
    print (f"Num ccs: { shell [0]. skel .num_connected_components()}")
    print (f"Some cc on all faces : { shell [0]. skel . is_some_cc_on_all_faces () }")

    # embedding and tiling
    side_len  = 1.0
    embedding = cuboid.embed(0.5*side_len, side_len , 2*side_len )
    tile  = Tile ( shell , embedding)
    pat  = Custom(Translate(cube. faces .FRONT, cube.faces.BACK, True,
                    Translate (cube. faces .BOTTOM, cube.faces.TOP, True,
                        Translate (cube. faces .LEFT, cube.faces .RIGHT, True))))
    return  Structure ( tile , pat)
```

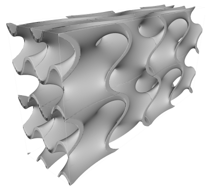

Figure 11: Example program and corresponding geometry for the implicit gyroid, with a stretched unit cell generated by embedding the Tile with a non-unit aspect ratio.

`UniformTPMSShellViaConjugation`), because the precise geometry is not known at the time of export; it is inferred by the ProcMeta kernel. As such, at this time, our simple kernel only supports SDF-based skeletons – e.g., those derived from `liftedSkelsFromSDF`. This could be expanded in the future.

To use our simple kernel to realize compatible MetaDSL structures, we wrote a new transpilation layer. This layer traverses the MetaDSL `Structure` object, and outputs a sequence of ordered operation nodes that match the interface given by our transpiler. This code is very similar to the transpiler required for ProcMeta.

Despite the simplicity of these extensions, they greatly expand the representative capacity of MetaDSL by incorporating the suite of implicit surfaces and other SDF based structures. Our simple, separate geometry kernel also relaxes one of the central limitations of ProcMeta: due to its simplicity, it does not need to make any assumptions about the form factor of the final structure. This permits translational units that reside in something other than a unit cube. Overall, this proof-of-concept demonstrates the capacity of MetaDSL to expand in a productive, non-breaking way.

B.6 Language Development Process and Insights

As mentioned in Appendix A.1, our geometry representation went through 3 major stages.

In the first iteration, we represented metamaterials using ProcMeta graphs directly. This had several issues: it was not compact enough for the context windows of small, lightweight models; intuitiveness and editability suffered dramatically without the aid of a GUI editing tool; the graphs' use of absolute coordinates proved challenging for LLMs (which struggle with spatial reasoning); and the program manipulations (e.g. hybridization, mutation) were unwieldy and fragile, with low validity rates that prohibited effective dataset scaling and diversification. This limited the breadth of MetaDB and MetaBench, while curtailing the efficacy of MetaAssist.

To address this, we designed a higher-level language that became MetaDSL-v0. This approach had a compact, modular, bilevel design that was embedded within Python and thus permitted semantically meaningful content; as such, it solved the context length and human editability issues of ProcMeta. It allowed for relative positioning, which mitigated the issues with coordinates while improving components' reusability. It also allowed for dataset augmentation through programmatic mutation, and improved the efficacy of VLM-based hybridization and mutation – we attributed this jump to our Python embedding, as VLMs show great facility with Python. Still, MetaDSL-v0 remained fragile: generated programs frequently failed, and database augmentations showed limited diversity.

	MetaDSL	ProcMeta
Compactness	**Shorter**, less boilerplate. Easier to read, less likely to exceed token limits	Longer, more boilerplate. Exceeds context of small, lightweight models.
Modules	**Highly reusable**. Patterns defined in composable chunks (eg TetMirror), independent of tile contents. Skeletons defined independent of embedding, easily scale to different Tiles.	**No support.** Limited reuse. Patterns can't exist independently; no pre-built Patterns. Absolute Skeletons, cannot easily be rescaled.
Relative vs. Absolute Positioning	Positions and transforms use **local coordinates** (i.e. [0,1]) wrt named entities (`cuboid.edges.TOP_LEFT`) in abstract polytopes. Robust for generation, clear design space bounds, more intuitive.	Positions and transforms use **absolute coordinates**. Easily misaligned, difficult to visualize without plotting. Unsuitable for VLMs, which struggle with computation/spatial tasks.
BV representation	**Explicit BV with named, referenceable entities.** Facilitates verifiable parametric design, e.g., vertex constrained to given BV edge. Allows type/error checking.	**Implicit or Absent BV**: drawn as a visual aid in the GUI, but not represented/preserved in the graph. Never referenceable.
Type/Error checking	**Type/incidence tracking to ensure compatibility** – e.g. conjugate TPMS require a closed loop where every edge lies in a BV face, and every BV face contains at least 1 loop edge. This is known from our representation and verified by downstream operations. Helps determine valid substitutions for mutations, even when large changes are proposed, leading to greater diversity. Critical for complex patterning, to determine compatibility of proposed-adjacent faces.	**None.** The burden of verification (for e.g. vertices on BV edges or edges in BV faces) is left to the user – infeasible for agentic design. Bad inputs crash ProcMeta with no explanation or suggested improvements.
Simplified Operations	**Abstractions simplify element creation**; e.g., Sphere() takes a center point and a radius, as one would expect. Easier for humans and LLMs.	Strict compliance with the given graph interface makes **some operations cumbersome**; e.g. for a sphere, thicken a 0-length edge chain over 2 co-located vertices
Semantic information	**Complete support.** Comments and meaningful variable names improve readability and admit metadata (provenance, parameter bounds)	No support.
Parameters	**Complete support.** Allows parametrized models and family generators.	**None.** Explicit positions etc. only. Variations defined as separate graphs. Difficult/impossible to infer constraints or design space from the graph description.
Loops, Functions	**Supports complex logic** that would be tedious to implement otherwise. Functions are especially useful for hybridization, as programs can be directly reused and/or rescaled.	**No support.** Each instance must be created/connected individually. Even hybridization is difficult, because subgraphs cannot be inserted directly – the identifier/references of each node must be updated.

Table 2: Detailed differences between the interfaces for MetaDSL and ProcMeta.

Analysis of MetaDSL-v0's failure modes offered several insights; we arrived at the current MetaDSL by addressing each in turn. First, we noticed that VLMs often used hallucinated synonyms, such as `TOP_LEFT` vs `LEFT_TOP`; we added overloads for all reasonable variations of our functions and attributes. We also found that it was critical to abrogate as much spatial reasoning from the VLM as possible: a full 1/3 of failures were due to the VLM's improper positioning of vertices that form the concrete polytope tiles. We circumvented this through abstracted tile embedding functions, which generate valid embeddings from simple, meaningful parameterizations. In our final large-scale change, we swapped the relative order of lifting functions and tile embeddings (previously Embed then Lift; now, Lift then Embed). This change improved the modularity and compositionality while reducing verbosity – for example, this change allows multiple skeletons to reside in a shared Tile embedding, such that they can be patterned as a single unit. This change also paved the way for patterning of more diverse geometry-generation methods in future extensions. As a result, MetaDSL showed dramatic improvements in generation/mutation rates, and – in turn – significantly more diverse LLM-driven hybridizations.

C MetaDB

C.1 Database Layout

MetaDB is structured into 4 primary directories:

- literature: Literature references that are the sources for hand-authored models.
- models: MetaDSL programs and their outputs.
- generators: Programs that create and augment models
- benchmark: The MetaBench benchmark

Data items in MetaDB can reference other items by path. These paths are either absolute (start with a forward slash "/") or relative (no leading slash). Absolute paths are assumed to start at the root of the database structure. For example, a model may reference the paper that defined it in its sources as `/literature/....`

C.2 Provenance Information

Each Model in MetaDB starts with a triple-single-quote (`'''`) delimited yaml string called the header-block. This contains useful metadata about the program, including provenance information about how it was created, and what sources it draws on. Provenance information is recorded in two places in the header block.

The primary location is in the "sources" key. This is a dictionary where the keys are MetaDB paths to literature, models, or generators that are the source of this model. The secondary location is in `file_info`→`generator_info`. For models that are autogenerated via enumeration or augmentation this section contains a MetaDB path to the script that generated the file, the arguments that were passed into that script, and specific `structure_details` that specified this particular model.

C.3 Hybridization Implementation

We hybridized hand-authored models using calls to OpenAI's o4-mini model using a reasoning effort of "medium". For every pair and triplet of authored models, we used the following prompt template:

~~~
You have access to a DSL whose specification is as follows:
{ api_description }

I want you to help discover unique new programs. Do this by genetic crossover based on these
    parent Metagen DSL programs:

1)
``` python
{program 1 code}
~~~

2)
``` python
{program 2 code}


Combine relevant structural / logical features from each sample into one coherent DSL program.
Be sure to:
- Respect the DSL syntax strictly .
- Maintain correctness in the final structure definition .
- Keep the final program well-formed and ready to be run as a standard Metagen DSL generator.
- Provide minimal descriptive comments.

Return only the resulting code in a single code block.
```

where `api_description` is the MetaDSL API specification given in Appendix G, and the program code is listed excluding the header block.

C.4 Mutation Implementation

Our mutation strategy is orchestrated by a Python script that uses dynamic program analysis to identify possible swaps within a program (e.g., beam lifting procedure to shell lifting procedure) and then apply a subset of them according to user-specified probability distributions. The possible swaps are determined by comparing the preconditions for a particular target operation to the state of the seed `Structure` in question; if all preconditions are met, the swap is considered possible. For example, the seed structure shown in Figure 2(b) has a `UniformBeams` lifting function; however, based on the fact that the constituent skeleton forms a closed loop, that lifting function could be replaced with `UniformDirectShell`. However, it does *not* meet the preconditions for `UniformTPMSShellViaConjugation`, because that additionally requires that every vertex of the skeleton resides on a CP edge, which is *not* the case for our seed structure.

First, our script loads a DSL model from file and constructs the corresponding Structure object in memory. Then, it is able to modify the structure along 4 different axes. Two of the axes allow discrete adjustments: (1) switching any `Polyline` to a `Curve` or vice versa; and (2) selecting a different lifting procedure from the set of options compatible with the skeleton (as inferred by our type system). The remaining modification axes permit continuous variations: (3) repositioning a vertex within its CP element; and (4) selecting a different thickness specification for any lifting procedures. To generate a given variant, each modification axis was permitted with a pre-specified probability; we used $\mathrm{Pr} = 0.7$ for both discrete changes, $\mathrm{Pr} = 0.9$ for vertex perturbation, and $\mathrm{Pr} = 0.98$ for thickness perturbation. Once a given perturbation category was permitted, we looped over each opportunity for said modification within our structure specification, and evaluated a random number against the same respective probability to decide whether this specific instance should be modified or not. For example, with $\mathrm{Pr} = 0.7$ we allow `Polyline/Curve` swaps in the variant; then, each time a candidate `Polyline/Curve` is identified, we enact the swap with $\mathrm{Pr} = 0.7$. Once an instance has been approved, the specific replacement value was chosen at random from the appropriate set of options (if more than one available). The updated structure is then written to file using the `dslTranslator`, which writes a DSL model from a Structure object. Additional mutation procedures could be implemented to further increase the vawriety of resulting structures.

Provenance Information is stored in the `sources` section of each program's header block. This is a dictionary where the keys are database paths.

C.5 Material Properties

Our simulation provides the 6×6 elastic tensor C in Voigt notation, along with the compliance matrix, $S = C^{-1}$. From this, we extract 18 common material properties:

- E: Young's Modulus, Voigt-Reuss-Hill (VRH) average, relative to E_{base}.
- E_1, E_2, E_3: Directional Young's Moduli, relative to E_{base}
- G: Shear Modulus (VRH average), relative to E_{base}
- G_{23}, G_{13}, G_{12}: Directional Shear Moduli, relative to E_{base}
- ν: Poisson ratio (VRH average)
- $\nu_{12}, \nu_{13}, \nu_{23}, \nu_{21}, \nu_{31}, \nu_{32}$: Directional Poisson ratios
- K: Bulk modulus (VRH average), relative to E_{base}
- A: Anisotropy (universal anisotropy index)
- V: Volume Fraction.

C.6 Ensuring MetaDB Quality

MetaDB is founded on a strong basis of expert programs, including 50 hand-authored examples sourced from diverse, singularly-developed designs in metamaterial literature. This large, diverse collection of seeds is unique to MetaDB, as most large datasets are derived exclusively from a small set of procedural generators. For example, Xue et al. [2025] creates a database of 180k samples, 78% of which stem from variations of the topologies in Elastic Textures [Panetta et al., 2015]. The remaining 22% stem from similar generators for planar- and curved-shell structures [Liu et al., 2022, Sun et al., 2023a]. Because of the reliance on such generators, Xue et al. [2025] does not offer any representation of e.g. CSG-style structures like the Bucklicrystal of Babaee et al. [2013]. However, the bucklicrystal is part of our database, as shown in Figure 4(i), center). MetaDB also already includes Elastic Textures, and similar generators could be implemented for the remaining sources mentioned above.

To ensure that MetaDB only contains high-quality material definitions – even when automatically generating a large portion of our entries – material models are only added after they have passed a series of basic checks. Presently, this includes 3 criteria:

- **MetaDSL compilation:** the model must contain valid python code that successfully evaluates to a MetaDSL Structure object. This includes all runtime type checking done by MetaDSL.
- **Valid Geometry Generation:** after the MetaDSL Structure object is transpiled into the target geometry kernel (in our case, ProcMeta), the kernel is run. We check the resulting geometry for validity, as measured by a non-null result that is tilable in 3D. To determine tilability, we tile the base cell in a $3 \times 3 \times 3$ lattice, then check that the boundaries are periodic and that at least one connected component of this larger base cell reaches all boundaries.
- **Physically Consistent Simulation Results:** the simulator must return reasonable results that obey physical constraints. For example, since our simulation is normalized by the base material's Young's modulus E_{base}, it must be the case that our simulation returns $E \leq 1$.

D Further Benchmark Results

D.1 Expanded Quantitative Results

In this section we extend the primary table from the paper Table 1 to include 95% confidence intervals, computed using the standard-error approximation (Table 3). We also show more detailed tables for each task category, broken down to the individual task type. These extended views do not change the primary observations from the main text, but do highlight the differences between subtasks.

Category	Inverse Design		Material Understanding		Reconstruction		
Metric	Error	Valid	Error	Valid	CD	IoU	Valid
Model							
LLaVAOmniTask	**0.011 ± 0.002**	**91.9% ± 0.9%**	0.024 ± 0.004	**100.0% ± 0.0%**	0.034 ± 0.001	0.490 ± 0.008	82.9% ± 0.9%
LLaVASingleTask	0.036 ± 0.007	81.9% ± 3.2%	**0.018 ± 0.004**	**100.0% ± 0.0%**	**0.029 ± 0.003**	**0.524 ± 0.030**	83.8% ± 3.2%
NovaLite	0.060 ± 0.023	2.7% ± 0.6%	0.200 ± 0.005	**100.0% ± 0.0%**	0.119 ± 0.003	0.051 ± 0.003	19.3% ± 0.9%
NovaOmniTask	0.026 ± 0.002	91.4% ± 1.0%	0.032 ± 0.005	**100.0% ± 0.0%**	0.045 ± 0.001	0.334 ± 0.007	**87.2% ± 0.8%**
NovaSingleTask	0.032 ± 0.007	79.2% ± 3.4%	0.153 ± 0.006	**100.0% ± 0.0%**	0.059 ± 0.003	0.205 ± 0.020	84.8% ± 3.2%
OpenAIO3	0.038 ± 0.006	24.7% ± 1.5%	0.077 ± 0.005	**100.0% ± 0.0%**	0.053 ± 0.001	0.147 ± 0.004	54.6% ± 1.1%

Table 3: Benchmark summary with confidence intervals.

Task	1 View			2 View			3 View			4 View		
Metric	CD	IoU	Valid	CD	IoU	Valid	CD	IoU	Valid	CD	IoU	Valid
Model												
LLaVAOmniTask	**0.036**	**0.458**	82.3%	**0.033**	**0.497**	83.0%	**0.032**	**0.509**	83.2%	0.033	0.497	83.2%
LLaVASingleTask	—	—	—	—	—	—	—	—	—	**0.029**	**0.524**	83.8%
NovaLite	0.119	0.049	18.7%	0.117	0.050	17.0%	0.118	0.053	22.0%	0.125	0.050	25.0%
NovaOmniTask	0.047	0.307	**87.5%**	0.044	0.338	**87.5%**	0.043	0.350	**86.2%**	0.044	0.346	**87.8%**
NovaSingleTask	—	—	—	—	—	—	—	—	—	0.059	0.205	84.8%
OpenAIO3	0.052	0.150	36.8%	0.055	0.141	58.9%	0.052	0.151	62.6%	0.052	0.155	68.5%

Table 4: Reconstruction Results Broken Down by task type.

Significance In Table 3 we show 95% confidence intervals around the sample means for our top-level task categories. From these we can see that for every task that LLaVASingleTask outperformed LLaVAOmniTask, the confidence intervals actually overlap, indicating that this performance boost from single-task training may not be significant. This reaffirms our decision to base our metamaterial co-pilot on the OmniTask trained models.

Categorical Results Tables 4, 5, and 6 break down Table 1 for each task category into its task variations (number of views, targets, etc.). These provide a more even point of comparison between single and omni-task models because the results are aggregated over exactly the same examples. By contrast, in the primary table, the omni-task models are averaging over more and different tasks; thus, they may be biased by overall easier or harder requests.

In reconstruction (Table 4), we see a trend that having more viewpoints makes reconstruction slightly easier. We can see that the inclusion of these harder tasks did pull down the OmniTask average slightly in the general benchmark, but it was not the deciding factor. A similar trend is seen in Nova, but there the gap is significantly larger.

For the inverse design tasks in Table 5, the 2 or 3 target design appears to be the easiest benchmark, depending on the model; however, there is not a clear trend stating whether more-or-fewer targets is easier. It is not clear why these intermediate task numbers are less difficult than single target design. Our hypothesis is that the individual targets become easier to achieve with increasing target count (either due to profile selection bias or correlation between targets in the real materials we are sampling from), but this is eventually counteracted by having more optimization criteria. More in-depth study is required to deduce why this happens.

The expanded material understanding results shown in Table 6 reveal only that predicting material properties with limited information (a single view), is somewhat more challenging than with an abundance of signal (many views and a MetaDSL representation); this is an unsurprising finding. This discrepancy did lower the overall accuracy of LLaVAOmniTask, but not enough to make a categorical difference.

Task	1 Target		2 Target		3 Target		4 Target		5 Target		6 Target	
Metric	Error	Valid	Error	Valid	Error	Valid	Error	Valid	Error	Valid	Error	Valid
Model												
LLaVAOmniTask	0.023	**99.0%**	**0.011**	**94.3%**	**0.007**	**93.1%**	**0.010**	89.7%	**0.008**	88.3%	**0.008**	87.9%
LLaVASingleTask	—	—	—	—	—	—	0.036	81.9%	—	—	—	—
NovaLite	0.036	2.1%	0.049	4.6%	0.043	2.0%	0.078	3.2%	0.083	1.2%	0.072	2.8%
NovaOmniTask	**0.020**	90.3%	0.018	90.6%	0.024	90.5%	0.029	**92.7%**	0.035	**90.2%**	0.028	**94.0%**
NovaSingleTask	—	—	—	—	—	—	0.032	79.2%	—	—	—	—
OpenAIO3	0.045	30.5%	0.035	20.2%	0.023	23.1%	0.045	20.5%	0.037	28.2%	0.042	25.9%

Table 5: Inverse Design Results broken down by task type.

Task	1 View		4 View + Code	
Metric	Error	Valid	Error	Valid
Model				
LLaVAOmniTask	**0.026**	**100%**	0.023	**100%**
LLaVASingleTask	—	—	**0.018**	**100%**
NovaLite	0.208	**100%**	0.192	**100%**
NovaOmniTask	0.031	**100%**	0.032	**100%**
NovaSingleTask	—	—	0.153	**100%**
OpenAIO3	0.084	**100%**	0.071	**100%**

Table 6: Material Understanding results broken down by task type.

D.2 Result Galleries

We also present randomly[2] sampled queries for each task, and visualize their results across models, along with their benchmark metrics. This shows the qualitative differences between the models' performances, while grounding the numeric metrics to make them more understandable.

Figure 12 illustrates reconstruction from 4 viewpoint renders. Of particular interest is the o3 column on the far right. For 4/5 examples, o3 correctly reproduced the basic shape of the side-on views up-to the number of repeats. This suggests that it can correctly build skeletons, but struggles with selecting the correct embedding scale.

Figure 13 illustrates material prediction based on specified property requirements. In these examples, the LLaVA models successfully generate materials that meet the given criteria, but other models occasionally generate invalid materials or fail to satisfy the specified requirements.

Figure 14 illustrates generated materials' predicted versus actual properties. In these examples the LLaVA and OmniTask Nova models do quite well, but single task Nova and untuned models (Novalite and o3) fall behind.

E MetaBench

E.1 Intermediate Representation

Each dataset is given by a set of .jsonl files: one file each for train, validate, and test. Each line of a .jsonl file describes a single example using a dictionary with the following keys:

- **'task_type'**: a string identifying the task category; in our case, it is one of {'reconstruction', 'inverse_design', 'material_understanding'}.
- **'label'**: unique text label identifying this task entry, using descriptive elements where applicable, such as provided image viewpoints or source files.
- **'source'**: [if applicable] path to the source metamaterial, relative to the database root (and including the leading '/')
- **'data'**: any and all data required to run evaluations, including references for large elements (e.g. images, meshes, etc.) and/or directly embedded values.
- **'query'**: natural language framing of the question to be provided to an LLM. Any images (or other non-text input) must be specified by reference.
- **'response'**: [optional] an expected response from an LLM that has been asked 'query'. This field is permitted to exist for a test example; removal of this information is the responsibility of the LLM-specific formatters, when required.

The system prompt has been purposefully excluded, both because it would be very large, and because that is an implementation detail of a predictive model, and not part of the benchmark itself.

E.2 Task Construction for Inverse Design

Inverse design tasks are specified as a collection of target values or bounded-ranges for a subset of material properties, from which we construct a natural-language query that describes that set of targets. Creating these tasks has two stages: selecting a set of targets, and generating an grammatically correct English sentence from those targets.

[2]rejection filtered so that all models had valid outputs for the input, except for inverse design where this was not possible

Input	**Predicted renderings**
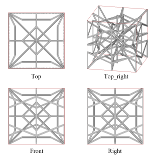	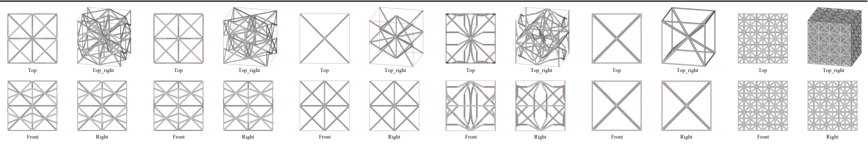

LLaVASingle	LLaVAOmni	NovaSingle	NovaOmni	NovaLite	OpenAI-o3
IoU: **0.417**	IoU: 0.218	IoU: 0.224	IoU: 0.071	IoU: 0.203	IoU: 0.078
CD: **0.032**	CD: 0.053	CD: 0.076	CD: 0.051	CD: 0.072	CD: 0.033

Input	**Predicted renderings**
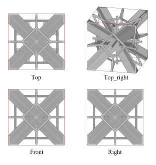	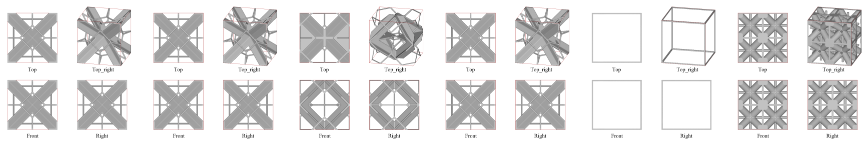

LLaVASingle	LLaVAOmni	NovaSingle	NovaOmni	NovaLite	OpenAI-o3
IoU: **0.838**	IoU: 0.838	IoU: 0.117	IoU: 0.838	IoU: 0.023	IoU: 0.215
CD: **0.004**	CD: 0.004	CD: 0.047	CD: 0.004	CD: 0.158	CD: 0.024

Input	**Predicted renderings**
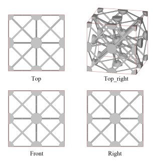	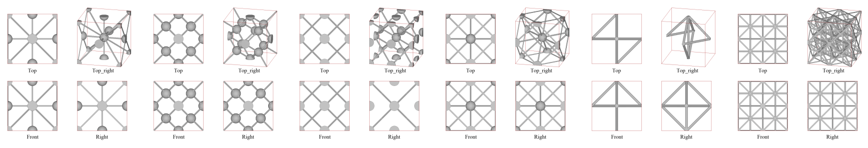

LLaVASingle	LLaVAOmni	NovaSingle	NovaOmni	NovaLite	OpenAI-o3
IoU: 0.307	IoU: 0.189	IoU: 0.463	IoU: **0.497**	IoU: 0.105	IoU: 0.426
CD: 0.073	CD: 0.081	CD: 0.032	CD: 0.053	CD: 0.107	CD: **0.018**

Input	**Predicted renderings**
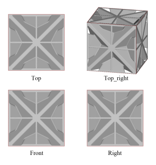	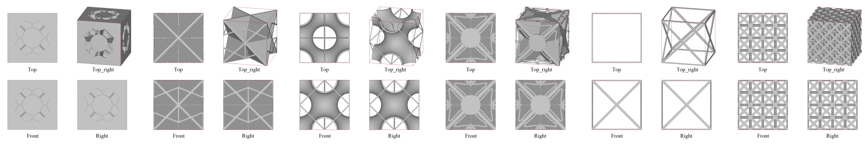

LLaVASingle	LLaVAOmni	NovaSingle	NovaOmni	NovaLite	OpenAI-o3
IoU: 0.296	IoU: 0.469	IoU: 0.078	IoU: **0.570**	IoU: 0.052	IoU: 0.280
CD: 0.022	CD: 0.014	CD: 0.051	CD: **0.011**	CD: 0.078	CD: 0.017

Input	**Predicted renderings**
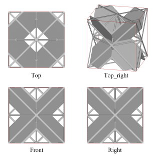	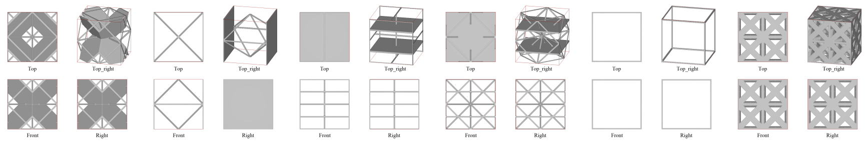

LLaVASingle	LLaVAOmni	NovaSingle	NovaOmni	NovaLite	OpenAI-o3
IoU: **0.745**	IoU: 0.049	IoU: 0.068	IoU: 0.067	IoU: 0.011	IoU: 0.096
CD: **0.015**	CD: 0.103	CD: 0.066	CD: 0.067	CD: 0.174	CD: 0.049

Figure 12: 4 View reconstruction results for random test samples by model. Left: the input renders shown to each model. Right: renders of predicted reconstructions.

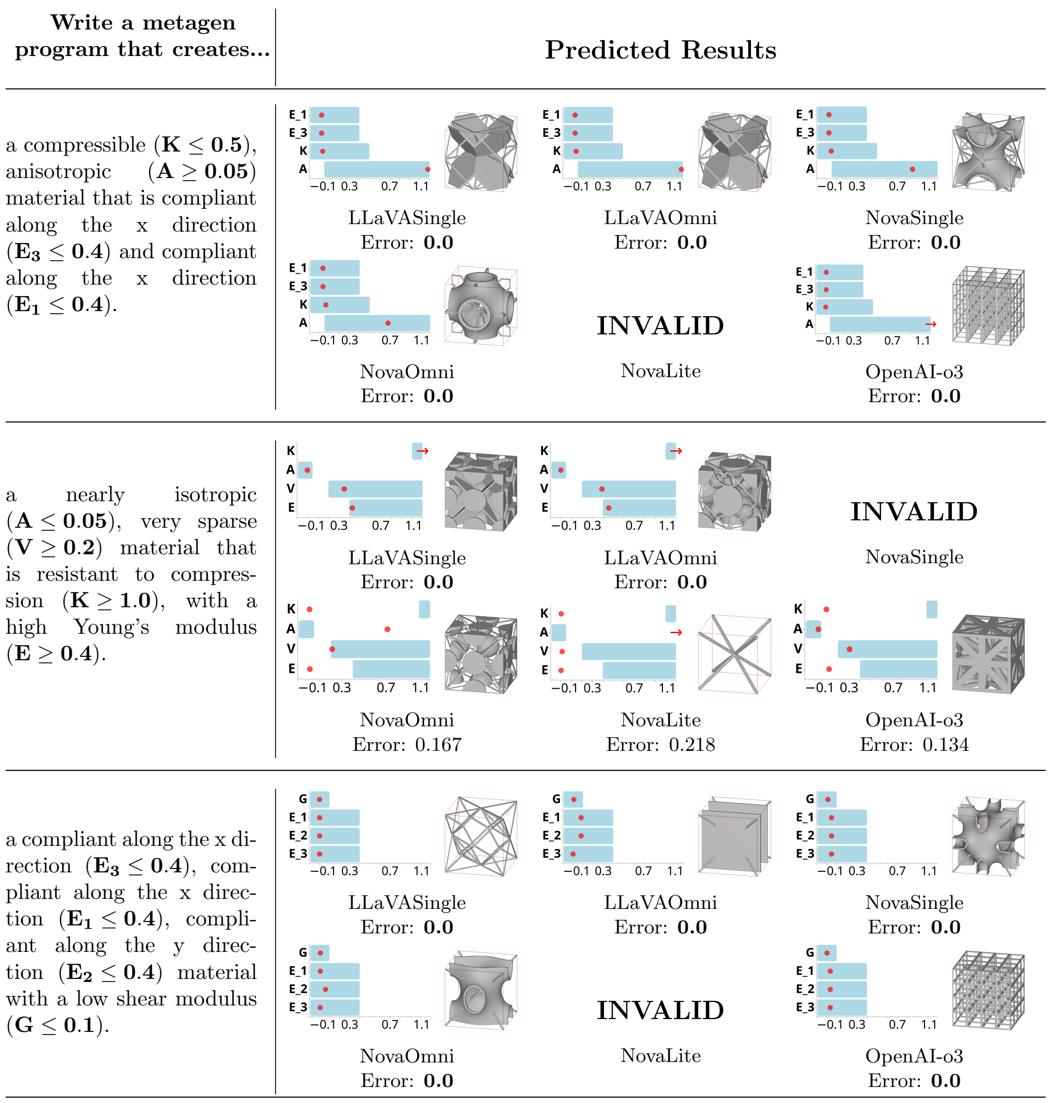

Write a metagen program that creates...

a compressible ($\mathbf{K} \leq \mathbf{0.5}$), anisotropic ($\mathbf{A} \geq \mathbf{0.05}$) material that is compliant along the x direction ($\mathbf{E_3} \leq \mathbf{0.4}$) and compliant along the x direction ($\mathbf{E_1} \leq \mathbf{0.4}$).

a nearly isotropic ($\mathbf{A} \leq \mathbf{0.05}$), very sparse ($\mathbf{V} \geq \mathbf{0.2}$) material that is resistant to compression ($\mathbf{K} \geq \mathbf{1.0}$), with a high Young's modulus ($\mathbf{E} \geq \mathbf{0.4}$).

a compliant along the x direction ($\mathbf{E_3} \leq \mathbf{0.4}$), compliant along the x direction ($\mathbf{E_1} \leq \mathbf{0.4}$), compliant along the y direction ($\mathbf{E_2} \leq \mathbf{0.4}$) material with a low shear modulus ($\mathbf{G} \leq \mathbf{0.1}$).

Figure 13: Inverse design results for a random selection of queries. Left: the text query given to each model. Right: paired data showing – for each model – an image of the generated structure alongside a property profile comparison. This profile shows the target values/ranges (in blue), versus simulated properties of the predicted materials (in red). Red arrows indicate that the predicted value is beyond the chart boundaries. Some models failed to produce a valid model for certain queries, indicated by the label "INVALID".

Input	Predicted Properties					
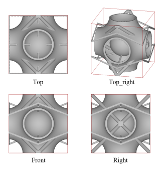	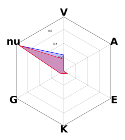 LLaVASingle Error: **0.007**	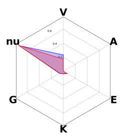 LLaVAOmni Error: 0.008	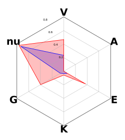 NovaSingle Error: 0.101	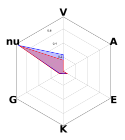 NovaOmni Error: 0.011	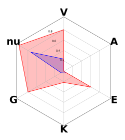 NovaLite Error: 0.233	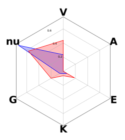 OpenAI-o3 Error: 0.062
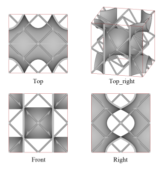	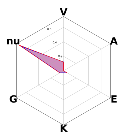 LLaVASingle Error: **0.003**	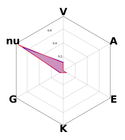 LLaVAOmni Error: 0.006	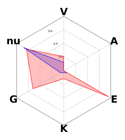 NovaSingle Error: 0.147	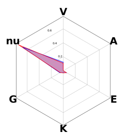 NovaOmni Error: 0.007	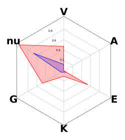 NovaLite Error: 0.162	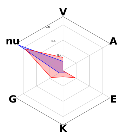 OpenAI-o3 Error: 0.043
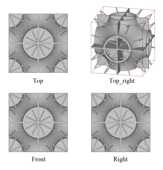	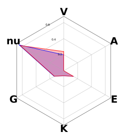 LLaVASingle Error: **0.006**	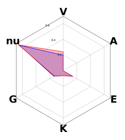 LLaVAOmni Error: 0.006	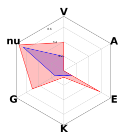 NovaSingle Error: 0.115	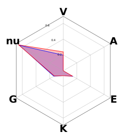 NovaOmni Error: 0.006	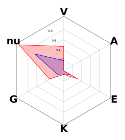 NovaLite Error: 0.088	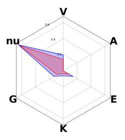 OpenAI-o3 Error: 0.020
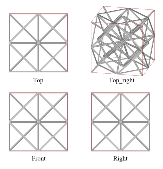	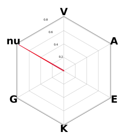 LLaVASingle Error: **0.000**	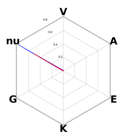 LLaVAOmni Error: 0.016	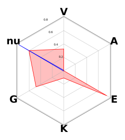 NovaSingle Error: 0.185	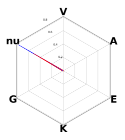 NovaOmni Error: 0.016	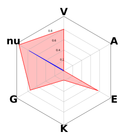 NovaLite Error: 0.276	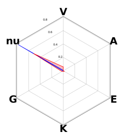 OpenAI-o3 Error: 0.024
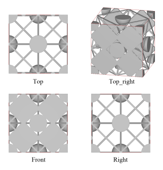	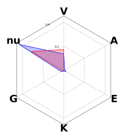 LLaVASingle Error: 0.014	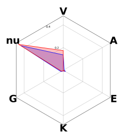 LLaVAOmni Error: **0.007**	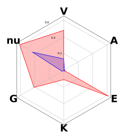 NovaSingle Error: 0.163	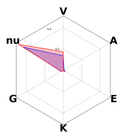 NovaOmni Error: 0.007	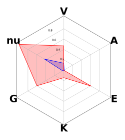 NovaLite Error: 0.209	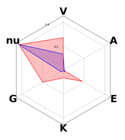 OpenAI-o3 Error: 0.056

Figure 14: Material property predictions given 4 input views (shown) and the program code (not shown). The radar charts plot the 6 averaged property values (scaled and shifted to always be positive). The blue regions show the ground truth values, while red shows the prediction.

Property References To aid in this process, we generate a reference dictionary with information about each of the 18 properties, of the following form:

```
{
'nu': {
    "full_prop_name": "Poisson ratio",
    "alternate_symbols": ["nu_{VRH}"],
    "property_generality": PropertyGenerality.OVERALL,
    "property_type": PropertyType.POISSON_RATIO,
    "dataset_coverage": {
        "min": -0.5,
        "max": 0.5,
        "q1": 0.3,
        "q3": 0.36,
        "densely_populated_ranges": [[0.2, 0.4]]
    },
    "smallest_meaningful_quantization": 0.01,
    "adjective_descriptors":[{"description": f"auxetic", "target_type": TargetType.
         UPPER_BOUND, "target_value":0}],
    "property_descriptors": [{"description": f"a negative Poisson ratio", "target_type":
         TargetType.UPPER_BOUND, "target_value":0},
                             {"description": f"a positive Poisson ratio", "target_type":
                                  TargetType.LOWER_BOUND, "target_value":0}],
    "verb_descriptors":      [{"description": f"contracts transversely under axial compression", "
          target_type": TargetType.UPPER_BOUND, "target_value":0},
                             {"description": f"expands transversely under axial compression", "
                                  target_type": TargetType.LOWER_BOUND, "target_value":0},
                             {"description": f"contracts in other directions when compressed
                                  along one axis", "target_type": TargetType.UPPER_BOUND, "
                                  target_value":0},
                             {"description": f"expands in other directions when compressed along
                                  one axis", "target_type": TargetType.LOWER_BOUND, "
                                  target_value":0},
                             {"description": f"expands transversely under axial elongation", "
                                  target_type": TargetType.UPPER_BOUND, "target_value":0},
                             {"description": f"contracts transversely under axial elongation", "
                                  target_type": TargetType.LOWER_BOUND, "target_value":0},
                             {"description": f"expands in other directions when stretched along
                                  one axis", "target_type": TargetType.UPPER_BOUND, "
                                  target_value":0},
                             {"description": f"contracts in other directions when stretched along
                                  one axis", "target_type": TargetType.LOWER_BOUND, "
                                  target_value":0}]
},
}
```

The full listing for all 18 properties is available in the metagen code provided in the supplement: `metagen/benchmarks_inverse_design.py`.

These entries provide information about the property ranges, dataset coverage, and interesting value breakpoints together with phrases that might be used to request them (e.g., "auxetic" implies $\nu < 0$). All aspects of these reference entries will be used in the following subsections to construct robust, varied and meaningful property queries for different material examples.

Active Property Selection For a given structure, we enforce that the "active" property subset follows two rules. First, the active set may only employ the overall values *or* the directional values for any given property – e.g., if a profile includes measure(s) for Young's modulus, it may either include the overall Young's modulus E *or* one or more of the directional values $\{E_1, E_2, E_3\}$; however, it is not permitted to simultaneously include E and one or more directional variants. Moreover, a profile is only allowed to use directional variants if it is sufficiently anisiotropic. We chose our anisotropy threshold as $A \geq 0.0025$, based on a manual exploration of the correlation between material spheres and anisotropy values appearing in our dataset. Subject to these rules, we select the "active" subset of properties based on a heuristic that determines the most interesting or salient properties of a given model.

We construct this heuristic score by examining individual properties of a model, and assigning a reward or penalty based on the expected notability of a particular characteristic or combination thereof. For example, if a material is near isotropic ($A < 0.0025$), we strongly reward the anisotropy property (so it is likely to end up in the active set) and heavily penalize all directional properties (so they will not be activated, as they are not likely to be notable). If the material is sufficiently anisotropic, we look at each property with directional variants, then compute pairwise differences between the values (e.g. E_1 vs. E_2). The directional properties are rewarded proportionally to each pairwise difference, so directions with larger discrepancies are more likely to be activated. Independently, we examine the ratio between the Young's modulus E and the volume fraction V – if the ratio is high (i.e., the material preserves stiffness with dramatically less material / lighter weight, which is a highly sought after combination), we strongly reward both properties. Finally, we examine each property in turn, and award additional points if they exhibit values that are extreme and/or underrepresented in our dataset. The reward is proportional to the relative extremity and inversely proportional to representation.

Given these scores, we iteratively select the highest-reward properties that preserve our overall active set rules. To ensure some variation in our inverse design profiles, we also introduce the opportunity to add randomly chosen properties into our profile: after each active set addition from the ranked data, we break the loop with some low probability (10%) and fill the remaining slots with randomly chosen properties that respect the rules relative to our partial active set.

Active Property Target Selection For each active property, we must now select a target value or range. To do this, we evaluate the options present in our reference dictionary, and extract all targets that are satisfied by the material at hand. We organize these into groups based on value and target type (range, value, lower/upper bound). Then, we choose the group that offers the tightest bound relative to the current material's property value. If multiple bound types are associated with the chosen target value, we select a bound type at random. Finally, we construct a profile with all targets matching the selected value and bound type. Assuming an example material where the Poisson ratio $\nu = -0.1$, the resulting profile might be as follows:

```
{
    "property": "nu"
    "target_value": 0
    "target_type": "upper_bound"
    "target_descriptions": [
        {
            "description": "auxetic",
            "description_type": "adjective"
        },
        {
            "description": "a negative Poisson ratio",
            "description_type": "noun"
        },
        {
            "description" : "contracts transversely under axial compression",
            "description_type": "verb"
        },
        {
            "description" : "contracts in other directions when compressed along one axis",
            "description_type": "verb"
        },
        {
            "description" : "expands transversely under axial elongation",
            "description_type": "verb"
        },
        {
            "description" : "expands in other directions when stretched along one axis",
            "description_type": "verb"
        }
    ]
}
```

Query Construction We want to create varied sentence structures to train and test against. To do this, each target type (value, upper bound, or lower bound) and target property has associated with it several descriptive phrases, as shown in the profile above. These phrases are paired with a part of speech (adjective, noun, or verb). As examples "very dense" (adjective), "contracts in the X direction when the Y direction is stretched" (verb), or "a negative Poisson ratio in at least one direction" (noun). Phrases that do not include numeric targets are accompanied by a parenthetical aside given a target value or range (e.g. "very dense (V > 0.8)."

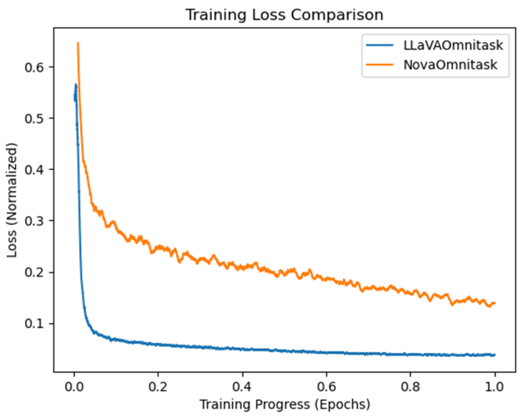

Figure 15: Training loss for LLaVAOmnitask and NovaOmnitask. Losses have been normalized so that starting-loss was 1. The LLaVA model converged very quickly, whereas the Nova loss was still decreasing. Given more training iterations or a steeper learning rate, is is possible that Nova performance would rise to match LLaVA's.

We start by randomly selecting one phrase for each target property, binning them by part of speech, then randomizing the order within bins. Adjectives are further randomly split between *front-adjectives* that precede the noun "material" ("a very dense material") and *back-adjectives* that follow it ("a material that is very dense"). We then form a query string by applying the template:

```
Write a metagen program that creates [a/an] { front_adjectives } material { back_adjectives } {verbs}
    {nouns}.
```

The template strings are augmented with part-of-speech appropriate connectors ("that is", "with", "that", "and"), and commas, depending on the parts of number of each part of speech in each position. The pronoun (a/an) as selected based on the first letter of `{front_adjectives}` if there are any, otherwise "a" for "a material".

F Implementation Details

LLaVASingleTask and LLaVAOmniTask tune Llama3-LLaVA-Next-8b Li et al. [2024], Liu et al. [2024] using low-rank adaptation Hu et al. [2022], with with $r = 16$ and $\alpha = 32$. Models were optimized using AdamW Loshchilov and Hutter [2017] with a 1e-5 learning rate and a cosine learning rate scheduler with 0.03 warm-up ratio. SingleTask models were trained on for 7000 iterations on 8 NVIDIA A100 GPUs over approximately 17 hours, while the OmniTask model was trained for just 1 epoch on 8 H200 GPUs over 25 hours due to its significantly larger training set, and for parity with the NovaLiteOmniTask. All LLaVA models were trained with a batch size of 16. During inference, the temperature was set to 0 to ensure deterministic outputs.

For commercial models we primarily used their default settings to avoid excess costs in hyperparameter tuning. NovaSingleTask models were trained on Amazon Bedrock with default settings (2 epochs, learning rate 1e-5, batch size 1, 10 learning rate warmup steps), and NovaOmniTask was trained with the same settings for 1 epoch. NovaSingleTask models trained for 4 hours for reconstruction and material understanding, and 2 hours for inverse design. The NovaOmniTask trained for 24 hours. Default Bedrock parameters were also used at inference time (temperature=0.7, topP=0.9, topK=50). OpenAI's o3 model was queried using the default "medium" reasoning level.

F.1 Training Curves

The surprising result that the smaller LLaVA models generally outperformed their much larger Nova counterparts is likely due to the smaller models converging more quickly given the same number of training examples.

F.2 Timing and Costs

MetaDSL execution and simulation time dominate LLM inference time for material generation. These are highly variable based on the geometric complexity of the generated program, with the majority executing and simulating in 5 minutes or less. MetaAssist generations are on average more time-complex that MetaDB (see Table 7. In practice, MetaAssist latencies are much lower because we do not run simulations in the interactive system.

Program Source	Avg. (s)	Median (s)	Std (s)
MetaDB	181	123	328
MetaAssist	591	290	746

Table 7: MetaDSL Execution and simulation times for program in MetaDB, and programs generated by MetaAssist using NovaOmni over the MetaBench test set (reconstruction and inverse design).

Since MetaDSL is quite compact, inference can be performed efficiently with few tokens. The majority of the inference tokens are taken by the common API-description system prompt (Appendix G.1), the cost of which can be amortized by caching. Using NovaOmni (ignoring caching for simplicity), the average MetaBench query used 8730 tokens (8284 input and 446 output). At current API pricing, the average query would cost $0.0006, and inference for the full test set would cost $7.11.

G Query Templates

For training models and running inference, we used prompt templates and inserted details for each specific query. In the following templates, `<[ ... ]>` is used as a delimiter to denote the inclusion of an image.

G.1 Universal System Prompt

For consistency, every example was provided with a common system prompt that describes the Metagen DSL, explains the material properties and rendered views we have in our dataset, and describes the basic task categories.

```
You are an expert metamaterials assistant that generates and analyzes cellular metamaterial
        designs based on material properties, images, and programatic definitions in the Metagen
        metamaterial DSL.


# Procedural Description in a Metamaterial DSL:

{ api_description }

# Material Analysis:
You can analyze the density, anisotropy, and elasticity properties of metamaterials. All
        metamaterials are assumed to be constucted from an isotropic base material with Poisson's
        ratio nu = 0.45.
The Young's Modulus of this base material is not specified, instead, the elastic moduli of the
        metamaterials -- Young's Modulus (E), Bulk Modulus (K), and Shear Modulus (G), are expressed
        relative to the base material Young's modulus (E_base). This means, for example, that
        relative Young's Moduli can range from 0 to 1. The material properties you can analyze are:

- E: Young's Modulus, Voigt-Reuss-Hill (VRH) average, relative to E_base
- E_1,E_2,E_3: Directional Young's Moduli, relative to E_base
- G: Shear Modulus (VRH average), relative to E_base
- G_23,G_13,G_12: Directional Shear Moduli, relative to E_base
- nu: Poisson ratio (VRH average)
- nu_12, nu_13, nu_23, nu_21, nu_31, nu_32: Directional Poisson ratios
- K: Bulk modulus (VRH average), relative to E_base
- A: Anisotropy (universal anisotropy index)
- V: Volume Fraction

# Material Images:

Images of metamaterials depict a base cell of the material rendered from four viewpoints:

- from the top
- from the front side
- from the right side
- from an angle at the upper-front-right

# Tasks:
```

```
You will be asked to perform several kinds of tasks:

– Reconstruction: from one or more images of a target material, reconstruct a Metagen program that
      generates the metamaterial in the images.
– Inverse Design: from a description of the properties of a desired materials, write a Metagen
      program that creates a metamaterial with those properties.
– Material Understanding: from images of a metamaterial and/or a Metagen program, analyze a
      material and predict its properties.
```

G.2 MetaDSL API

The Metagen language description (inserted as the `api_description` in the system prompt above) is as follows:

```
Programs in Metagen are built in two stages: one that creates local geometric structure, and a
      second that patterns this structure throughout space. Each of these is further broken down
      into subparts.


===================================
   API description (Boilerplate)
===================================
Each program is given as a python file (.py).
This program must import the metagen package and define a function called "make_structure()",
      which returns the final Structure object defined by the program.
If parameters are present in make_structure(), they MUST have a default value.
Specifically, the file structure is as follows:


from metagen import *

def make_structure(...) -> Structure:
   <content>




===================================
   DSL description
===================================

======= Skeleton Creation ========
vertex(cpEntity, t)
   @description:
      Create a new vertex. This vertex is defined relative to its containing convex polytope (
         CP). It will only have an embedding in R3 once the CP has been embedded.
   @params:
      cpEntity     – an entity of a convex polytope (CP), referenced by the entity names.
      t            – [OPTIONAL] list of floats in range [0,1], used to interpolate to a specific
         position on the cpEntity.
                     If cpEntity is a corner, t is ignored.
                     If cpEntity is an edge, t must contain exactly 1 value. t is used for
                        linear interpolation between the endpoints of cpEntity.
                     If cpEntity is a face, t must contain exactly 2 values. If cpEntity is a
                        triangular face, t is used to interpolate via barycentric coordinates
                        . If cpEntity is a quad face, bilinear interpolation is used.

                     If the optional interpolant t is omitted for a non–corner entity, the
                        returned point will be at the midpoint (for edge) or the centroid (
                        for face) of the entity. Semantically, we encourage that t be
                        excluded (1) if the structure would be invalid given a different non
                        –midpoint t, or (2) if the structure would remain unchanged in the
                        presence a different t (e.g., in the case of a conjugate TPMS,
                        where only the entity selection matters).
   @returns:
      vertex       – the new vertex object
```

```
    @example_usage:
        v0 = vertex (cuboid.edges.BACK_RIGHT, [0.5])
        v1 = vertex (cuboid.edges.TOP_LEFT)


Polyline ( ordered_verts )
    @description:
        Creates a piecewise−linear path along the ordered input vertices . All vertices must be
             referenced to the same CP (e.g ., all relative to cuboid entities ). The resulting path
              will remain a polyline in any structures that include it .
    @params:
        ordered_verts      − a list of vertices , in the order you'd like them to be traversed . A
             closed loop may be created by repeating the zeroth element at the end of the list .
             No other vertex may be repeated . Only simple paths are permitted .
    @returns:
        polyline           − the new polyline object
    @example_usage:
        p0 = Polyline ([ v2, v3])
        p0 = Polyline ([ v0, v1, v2, v3, v4, v5, v0])


Curve( ordered_verts )
    @description:
        Creates a path along the ordered input vertices . This path will be smoothed at a later
             stage (e.g ., to a Bezier curve), depending on the lifting procedures that are chosen.
              All input vertices must be referenced to the same CP (e.g ., all relative to cuboid
              entities ) .
    @params:
        ordered_verts      − a list of vertices , in the order you'd like them to be traversed . A
             closed loop may be created by repeating the zeroth element at the end of the list .
             No other vertex may be repeated . Only simple paths are permitted .
    @returns:
        curve              − the new curve object
    @example_usage:
        c0 = Curve([v2, v3])
        c0 = Curve([v0, v1, v2, v3, v4, v5, v0])

skeleton ( entities )
    @description:
        Combines a set of vertices OR polylines / curves into a larger structure , over which
              additional information can be inferred . For example, within a skeleton , multiple
             open polylines / curves may string together to create a closed loop, a branched path ,
             or a set of disconnected components.
    @params:
        entities           − a list of entities ( vertices or polylines / curves) to be combined. A
             given skeleton must only have entities with the same dimension −− that is , it must
             consist of all points or all polylines / curves .
    @returns:
        skeleton           − the new skeleton object
    @example_usage:
        skel = skeleton ([ curve0, polyline1 , curve2, polyline3 ])
        skel = skeleton ([ v0])


======= Lifting Procedures ========
UniformBeams(skel, thickness )
    @description:
        Procedure to lift the input skeleton to a 3D volumetric structure by instantiating a beam
             of the given thickness centered along each polyline / curve of the input skeleton .
    @requirements:
        The skeleton must contain only polylines and/or curves . The skeleton must not contain any
             standalone vertices .
    @params:
        skel               − the skeleton to lift
        thickness          − the diameter of the beams
    @returns:
          liftProc              − the   lifted   skeleton
    @example_usage:
          liftProcedure   = UniformBeams(skel, 0.03)

SpatiallyVaryingBeams( skel ,    thicknessProfile  )
    @description:
         Procedure  to   lift   the  input   skeleton  to  a  3D volumetric   structure   by   instantiating   a  beam
                 of  the  given   spatially −varying  thickness   profile   centered  along  each  polyline /curve
                 of  the  input   skeleton .
    @requirements:
         The skeleton  must contain  only  polylines  and/or  curves .  The skeleton  must not  contain  any
                 standalone   vertices  .
    @params:
         skel                   − the   skeleton  to   lift
          thicknessProfile −   specifications   for  the  diameter  of  the  beams along each  polyline /curve .
                Given as  a   list [  list [  floats  ]],  where the  each  of  the  n  inner   lists   gives  the
                 information  for  a  single  sample point  along  the  polyline /curve .  The  first   element  in
                each  inner   list   provides  a  position  parameter  t \\ in [0,1]  along  the  polyline /curve ,
                and  the  second element  specifies   the  thickness  of  the  beam at  position  t
    @returns:
          liftProc              − the   lifted   skeleton
    @example_usage:
          liftProcedure   = SpatiallyVaryingBeams( skel ,  0.03)

UniformDirectShell ( skel ,   thickness )
    @description:
         Procedure  to   lift   the  input   skeleton  to  a  3D volumetric   structure   by   inferring   a  surface
                 that  conforms to  the  boundary provided  by  the  input   skeleton .  The surface   is   given  by
                  a  simple  thin   shell  model:  the   resulting   surface   is   incident  on  the  provided
                boundary while  minimizing a  weighted  sum of  bending  and   stretching   energies .  The
                boundary  is   fixed ,  though  it  may be  constructed  with  a  mix of  polylines  and curves  (
                which are   first   interpolated   into  a  spline ,  then  fixed  as  part  of  the  boundary).  The
                 skeleton  must contain  a  single  closed  loop  composed of one  or  more polylines  and/or
                curves .  The  skeleton  must not  contain  any  standalone   vertices  .
    @requirements:

    @params:
         skel                   − the   skeleton  to   lift
         thickness            − the   thickness  of  the   shell .  The  final   offset   is   thickness /2  to  each  side
                  of  the   inferred   surface .
    @returns:
          liftProc              − the   lifted   skeleton
    @example_usage:
          liftProcedure   = UniformDirectShell ( skel ,   0.1)

UniformTPMSShellViaConjugation(skel, thickness )
    @description:
         Procedure  to   lift   the  input   skeleton  to  a  3D volumetric   structure   by   inferring   a   triply
                 periodic  minimal  surface  (TPMS) that conforms to  the  boundary  constraints   provided  by
                  the  input   skeleton .  The surface   is   computed via  the  conjugate   surface   construction
                method.
    @requirements:
         The skeleton  must contain  a  single   closed  loop  composed of one  or  more polylines  and/or
                curves .  The  skeleton  must not  contain  any  standalone   vertices  .
         Each vertex  in  the   polylines /curves  must  live  on  a  CP edge.
         Adjacent   vertices   must have  a  shared  face .
         The loop  must touch  every  face  of  the  CP at  least  once.
          If  the  CP has N faces ,  the  loop  must contain  at  least  N  vertices .
    @params:
         skel                   − the   skeleton  to   lift
         thickness            − the   thickness  of  the   shell .  The  final   offset   is   thickness /2  to  each  side
                  of  the   inferred   surface .
    @returns:
          liftProc              − the   lifted   skeleton
    @example_usage:
        liftProcedure  = UniformTPMSShellViaConjugation(skel, 0.03)

UniformTPMSShellViaMixedMinimal(skel, thickness)
    @description:
        Procedure to lift the input skeleton to a 3D volumetric structure by inferring a triply
             periodic minimal surface (TPMS) that conforms to the boundary constraints provided by
             the input skeleton. The surface is computed via mean curvature flow. All polyline
             boundary regions are considered fixed, but any curved regions may slide within their
             respective planes in order to reduce surface curvature during the solve.
    @requirements:
        The skeleton must contain a single closed loop composed of one or more polylines and/or
             curves. The skeleton must not contain any standalone vertices.
        Each vertex in the polylines/curves must live on a CP edge.
        Adjacent vertices must have a shared face.
    @params:
        skel             - the skeleton to lift
        thickness        - the thickness of the shell. The final offset is thickness/2 to each side
             of the inferred surface.
    @returns:
        liftProc         - the lifted skeleton
    @example_usage:
        liftProcedure  = UniformTPMSShellViaMixedMinimal(skel, 0.03)

Spheres(skel, thickness)
    @description:
        Procedure to lift the input skeleton to a 3D volumetric structure by instantiating a
             sphere of the given radius centered at vertex p, for each vertex in the skeleton.
    @requirements:
        The skeleton must only contain standalone vertices; no polylines or curves can be used.
    @params:
        skel             - the skeleton to lift
        thickness        - the sphere radius
    @returns:
        liftProc         - the lifted skeleton
    @example_usage:
        s_lift  = Spheres(skel, 0.25)


======= Tile Creation ========
Tile( lifted_skeletons , embedding)
    @description:
        Procedure to embed a copy of the skeleton in R^3 using the provided embedding information.
             The embedding information can be computed by calling the "embed" method of the
             relevant CP.
    @requirements:
        The embedding information must correspond to the same CP against which the vertices were
             defined. For example, if the vertices are defined relative to the cuboid, you must
             use the cuboid.embed() method.
    @params:
        lifted_skeletons - a list of lifted skeleton entities to embed in R^3. All entities must
             reside in the same CP type, and this type must have N corners.
        embedding        - information about how to embed the CP and its relative skeletons within
             R^3. Obtained using the CP's embed() method
    @returns:
        tile             - the new tile object
    @example_usage:
        embedding = cuboid.embed(side_len, side_len, side_len, cornerAtAABBMin=cuboid.corners.
             FRONT_BOTTOM_LEFT)
        s_tile  = Tile([beams, shell], embedding)


======= Patterning Procedures ========
TetFullMirror()
    @description:
        Procedure which uses only mirrors to duplicate a tet−based tile such that it partitions R
             ^3
    @params:
        N/A
    @returns:
        pat       − the patterning procedure
    @example_usage:
        pat = TetFullMirror ()

TriPrismFullMirror ()
    @description:
        Procedure which uses only mirrors to duplicate a triangular prism−based tile such that it
             partitions R^3
    @params:
        N/A
    @returns:
        pat       − the patterning procedure
    @example_usage:
        pat = TriPrismFullMirror ()

CuboidFullMirror()
    @description:
        Procedure which uses only mirrors to duplicate an axis−aligned cuboid tile such that it
             fills a unit cube, such that it partitions R^3. Eligible cuboid CPs must be such
             that all dimensions are 1/(2^k) for some positive integer k.
    @params:
        N/A
    @returns:
        pat       − the patterning procedure
    @example_usage:
        pat = CuboidFullMirror()

Identity ()
    @description:
        No−op patterning procedure.
    @params:
        N/A
    @returns:
        pat       − the patterning procedure
    @example_usage:
        pat = Identity ()

Custom(patternOp)
    @description:
        Environment used to compose a custom patterning procedure. Currently only implemented for
             the Cuboid CP.
    @params:
        patternOp− outermost pattern operation in the composition
    @returns:
        pat       − the complete patterning procedure
    @example_usage:
        pat = Custom(Rotate180([cuboid.edges.BACK_RIGHT, cuboid.edges.BACK_LEFT], True,
                    Rotate180([cuboid.edges.TOP_RIGHT], True)))

Mirror( entity , doCopy, patternOp)
    @description:
        Pattern operation specifying a mirror over the provided CP entity , which must be a CP
             Face. Can only be used inside of a Custom patterning environment.
    @params:
        entity     − CP Face that serves as the mirror plane.
        doCopy   − boolean. When True, applies the operation to a copy of the input, such that the
             original and the transformed copy persist . When False, directly transforms the input
             .
        patternOp− [OPTIONAL] outermost pattern operation in the sub−composition, if any
    @returns:
        pat          − the  composed patterning  procedure ,  which may be used  as  is  ( within  the  Custom
             environment),  or  as  the  input  for  further  composition
  @example_usage:
        pat  = Custom(Mirror(cuboid. faces . TOP, True,
                            Mirror ( cuboid . faces . LEFT, True)))

Rotate180(  entities  ,  doCopy, patternOp)
  @description :
        Pattern  operation  specifying  a  180 degree  rotation  about  the  provided  CP entity .  Can only
             be  used  inside  of  a  Custom patterning  environment.
  @params:
        entities   − List  of  CP  entities ,  which define  the  axis  about which to  rotate .  If  a  single
              entity  is  provided ,  it  must be a  CP Edge.  If  multiple  entities ,  they  will  be used  to
              define  a  new  entity  that  spans  them.  For example,  if  you provide  two  corners ,  the
              axis  will  go from one  to  the  other .  If  you provide  two CP Edges,  the  axis  will  reach
             from  the  midpoint  of  one  to  the  midpoint  of  the  other .
        doCopy   − boolean .  When True,  applies  the  operation  to  a  copy of  the  input ,  such  that  the
                original  and the  transformed  copy  persist .  When False,  directly  transforms  the  input
             .
        patternOp−  [OPTIONAL] outermost pattern operation  in  the  sub−composition,  if  any
  @returns:
        pat          − the  composed patterning  procedure ,  which may be used  as  is  ( within  the  Custom
             environment),  or  as  the  input  for  further  composition
  @example_usage:
        pat  = Custom(Rotate180([cuboid.edges . FRONT_LEFT, cuboid.edges.FRONT_RIGHT], True))

Translate ( fromEntity ,   toEntity ,  doCopy, patternOp)
  @description :
        Pattern  operation  specifying  a  translation  that  effectively  moves the  fromEntity  to  the
              targetEntity  .  Can only  be  used  inside  of  a  Custom patterning  environment.
  @params:
        fromEntity− CP Entity  that  serves  as  the  origin  of  the  translation  vector .  Currently  only
             implemented for  a  CP Face.
        toEntity   − CP Entity  that  serves  as  the  target  of  the  translation  vector .  Currently  only
             implemented for  a  CP Face.
        doCopy   − boolean .  When True,  applies  the  operation  to  a  copy of  the  input ,  such  that  the
                original  and the  transformed  copy  persist .  When False,  directly  transforms  the  input
             .
        patternOp−  [OPTIONAL] outermost pattern operation  in  the  sub−composition,  if  any
  @returns:
        pat          − the  composed patterning  procedure ,  which may be used  as  is  ( within  the  Custom
             environment),  or  as  the  input  for  further  composition
  @example_usage:
        gridPat  = Custom(Translate ( cuboid . faces . LEFT, cuboid. faces . RIGHT, True,
                                      Translate ( cuboid . faces . FRONT, cuboid.faces.BACK, True)))


======= Structure Procedures  ========
Structure ( tile  ,   pattern )
  @description :
        Combines local  tile  information  ( containing  lifted  skeletons ) with  the  global  patterning
             procedure  to  generate  a  complete  metamaterial .
  @params:
        tile                 − the  tile  object ,  which has  (by  construction )  already  been embedded in 3
             D space,  along  with  all  lifted  skeletons  it  contains .
        pattern              − the  patterning  sequence to  apply  to  extend  this  tile  throughout  space
  @returns:
        structure            − the  new  structure  object
  @example_usage:
        obj  =  Structure ( tile  ,  pat )

Union(A, B)
  @description :
        Constructive  solid  geometry Boolean  operation  that  computes the  union  of  two  input
              structures  .  The output  of  Union(A,B) is  identical  to  Union(B,A)
```

```
      @params:
            A                     − the  first  Structure  to be unioned. This may be the output of Structure ,
                    Union, Subtract , or Intersect
            B                     − the second Structure  to be unioned. This may be the output of Structure ,
                    Union, Subtract , or Intersect
      @returns:
            structure           − the new structure  object  containing union(A,B)
      @example_usage:
            final_obj  = Union(schwarzP_obj, Union(sphere_obj , beam_obj))

Subtract (A, B)
      @description:
            Constructive  solid geometry Boolean operation  that computes the  difference (A − B) of two
                    input  structures . The relative  input order is  critical .
      @params:
            A                     − the  first  Structure , from which B will be subtracted . This may be the
                    output of Structure , Union, Subtract , or Intersect
            B                     − the second Structure , to be subtracted from A. This may be the output of
                    Structure , Union, Subtract , or Intersect
      @returns:
            structure           − the new structure  object  containing (A − B)
      @example_usage:
            final_obj  = Subtract (c_obj , s_obj )

 Intersect (A, B)
      @description:
            Constructive  solid geometry Boolean operation  that computes the  intersection  of two input
                    structures , A and B.
      @params:
            A                     − the  first  Structure , which may be the output of Structure , Union,
                    Subtract , or Intersect
            B                     − the second Structure , which may be the output of Structure , Union,
                    Subtract , or Intersect
      @returns:
            structure           − the new structure  object  containing the  intersection  of A and B
      @example_usage:
            final_obj  = Intersect (c_obj , s_obj )




===================================
      Prebuilt Convex Polytopes
===================================
There are 3 prebuilt convex polytopes (CP) available for use: cuboid, triPrism , and tet . Each CP
        comprises a set of Entities , namely faces , edges and corners .
For convenience, each individual entity can be referenced using the pattern <CP>.<entity_type>.<
        ENTITY_NAME>.
For example, you can select a particular edge of the cuboid with the notation cuboid.edges.
        BOTTOM_RIGHT.
Each CP also has an embed() method which returns all necessary information to embed the CP within
        R^3.

The full list of entities and embed() method signatures for our predefined CPs are as follows:

 tet . corners .{     BOTTOM_RIGHT,
                      BOTTOM_LEFT,
                      TOP_BACK,
                      BOTTOM_BACK
                }
 tet .edges.    {     BOTTOM_FRONT,
                      TOP_LEFT,
                      BACK,
                      BOTTOM_RIGHT,
                      TOP_RIGHT,
                    BOTTOM_LEFT
               }
tet . faces .  {    BOTTOM,
                    TOP,
                    RIGHT,
                    LEFT
               }
tet .embed(bounding_box_side_length)
    @description:
        Constructs the information required to embed the tet CP in R^3
    @params:
        bounding_box_side_length- length of axis-aligned bounding box containing the tet . Float in
              range [0,1]. Must be 1/2^k for some integer k
    @returns:
        embedding      - the embedding information. Specifically , the position in R^3 of all the
             CP corners.
    @example_usage:
        side_len = 0.5 / num_tiling_unit_repeats_per_dim
        embedding = tet .embed(side_len)


triPrism . corners .{ FRONT_BOTTOM_LEFT,
                    FRONT_TOP,
                    FRONT_BOTTOM_RIGHT,
                    BACK_BOTTOM_LEFT,
                    BACK_TOP,
                    BACK_BOTTOM_RIGHT
               }
triPrism .edges.{ FRONT_LEFT,
                    FRONT_RIGHT,
                    FRONT_BOTTOM,
                    BACK_LEFT,
                    BACK_RIGHT,
                    BACK_BOTTOM,
                    BOTTOM_LEFT,
                    TOP,
                    BOTTOM_RIGHT
               }
triPrism . faces .{ FRONT_TRI,
                    BACK_TRI,
                    LEFT_QUAD,
                    RIGHT_QUAD,
                    BOTTOM_QUAD
               }
triPrism .embed(bounding_box_side_length)
    @description:
        Constructs the information required to embed the triangular prism CP in R^3
    @params:
        bounding_box_side_length - length of axis-aligned bounding box containing the triangular
             prism. Float in range [0,1]. Must be 1/2^k for some integer k
    @returns:
        embedding      - the embedding information. Specifically , the position in R^3 of all the
             CP corners.
    @example_usage:
        side_len = 0.5 / num_tiling_unit_repeats_per_dim
        embedding = triPrism .embed(side_len)


cuboid. corners .{ FRONT_BOTTOM_LEFT,
                    FRONT_BOTTOM_RIGHT,
                    FRONT_TOP_LEFT,
                    FRONT_TOP_RIGHT,
                    BACK_BOTTOM_LEFT,
                    BACK_BOTTOM_RIGHT,
                    BACK_TOP_LEFT,
                    BACK_TOP_RIGHT
               }
cuboid.edges.{      FRONT_BOTTOM,
                    FRONT_LEFT,
                    FRONT_TOP,
                    FRONT_RIGHT,
                    BACK_BOTTOM,
                    BACK_LEFT,
                    BACK_TOP,
                    BACK_RIGHT,
                    BOTTOM_LEFT,
                    TOP_LEFT,
                    TOP_RIGHT,
                    BOTTOM_RIGHT
               }
cuboid.faces.{      FRONT,
                    BACK,
                    TOP,
                    BOTTOM,
                    LEFT,
                    RIGHT
               }

cuboid.embed(width, height, depth, cornerAtMinPt)
    @description:
        Constructs the information required to embed the cuboid CP in R^3
    @params:
        width          - length of cuboid side from left to right. float in range [0,1]. Must be
              1/2^k for some integer k
        height         - length of cuboid side from top to bottom. float in range [0,1]. Must be
              1/2^k for some integer k
        depth          - length of cuboid side from front to back. float in range [0,1]. Must be
              1/2^k for some integer k
        cornerAtMinPt  - CP corner entity (e.g., cuboid.corners.FRONT_BOTTOM_LEFT) that
              should be collocated with the cuboid's minimum position in R^3
    @returns:
        embedding      - the embedding information. Specifically, the position in R^3 of all the
              CP corners.
    @example_usage:
        side_len = 0.5 / num_tiling_unit_repeats_per_dim
        embedding = cuboid.embed(side_len, side_len, side_len, cornerAtAABBMin=cuboid.corners.
              FRONT_BOTTOM_LEFT)

cuboid.embed_via_minmax(aabb_min_pt, aabb_max_pt, cornerAtMinPt)
    @description:
        Constructs the information required to embed the cuboid CP in R^3
    @params:
        aabb_min_pt    - Minimum point of the cuboid, in R^3. Given as a list of length 3, where
              each component must be a float in range [0,1], with 1/2^k for some integer k
        aabb_max_pt    - Maximum point of the cuboid, in R^3. Given as a list of length 3, where
              each component must be a float in range [0,1], with 1/2^k for some integer k
        cornerAtMinPt  - CP corner entity (e.g., cuboid.corners.FRONT_BOTTOM_LEFT) that
              should be collocated with the cuboid's minimum position in R^3
    @returns:
        embedding      - the embedding information. Specifically, the position in R^3 of all the
              CP corners.
    @example_usage:
        side_len = 0.5 / num_tiling_unit_repeats_per_dim
        embedding = cuboid.embed([0,0,0], [side_len, side_len, side_len], cuboid.corners.
              BACK_BOTTOM_RIGHT)
```

API Errata The API description listed in this section is the exact version we used to train all models in MetaBench. This differs slightly from the released version, which corrects two mistakes that were identified at a later stage:

- `cuboid.embed()`: the original description (above) listed a parameter `cornerAtMinPt` in both the signature line and the `@params` listing. However, the `@example_usage` showed the parameter as `cornerAtAABBMin`. The latter is correct, and reflects an update made in the code independently of the documentation. The released API description consistently shows the correct parameter name, `cornerAtAABBMin`.
- `cuboid.embed_via_minmax()`: the `@example_usage` field of the original description (above) erroneously lists the `cuboid.embed()` function with the inputs of the intended function, `cuboid.embed_via_minmax()`. None of the parameters were updated, as they are all correct in the original description above. Only the erroneous function call was corrected in the released version (`cuboid.embed()` $\rightarrow$ `cuboid.embed_via_minmax()`).

These mistakes did not cause any observable issue in the trained model output, as the (correctly expressed) training data overrode the error in our API description. However, this did cause an issue for zero shot experiments (which ultimately revealed the bug). All zero shot results reported in the paper reflect the results using the *updated* version of our API, where the difference relative to the listing above constitutes exactly the two changes discussed here.

To ensure that this API description would not derail otherwise successful program outputs (and to mitigate confusion between the two very similar keywords across functions), we added an optional keyword argument to the signature of both affected functions, such that either keyword (or no keyword, as in a positional argument) is permissible. Thus, either API description is suitable; however, we release the corrected version to prevent issues and reduce confusion moving forward.

G.3 Reconstruction

Reconstruction tasks can have any combination of one to four views. Here we only reproduced the 4 view template; the others have the irrelevant lines removed.

~~~
# Task:
Analyze these views of a metamaterial, then generate a metamaterial DSL procedure to reproduce it.

# Inputs:
**Rendered Views:**
Top: <[{top}]>
Front: <[{front}]>
Right: <[{right}]>
Angled (Front-Top-Right): <[{top_right}]>

# Output Format:
Generate a Metagen program within a python code block:

```python
from metagen import *

def make_structure(...) -> Structure:
    ...
~~~
```

## G.4 Inverse Design

```
Task:
Write a metagen program that creates {query_target}.

Output Format:
Generate a Metagen program within a python code block:

```python
from metagen import *

def make_structure(...) -> Structure:
    ...
```
```
```

G.5 Material Understanding

Single View:

```
# Task:
Analyze these views of a metamaterial, and predict its material properties.

# Inputs:

**Rendered View:**

- Angled (Front-Top-Right): <[{ top_right }]>

# Output Format:

Output a json object, delimited by ```json ```, where the keys are material property names, and
    the values are the predicted material properties. Predict these properties (keys):
- "A" : Anisotropy ( universal anisotropy index)
- "E" : Young's Modulus relative to E_base
- "K" : Bulk modulus relative to E_base
- "G": Shear modulus relative to E_base
- "nu": Isotropic Poisson ratio
- "V" : Relative Density (Volume Fraction)
```

Multiview + Code:

```
# Task:
Analyze these views of a metamaterial, and the Metagen program, and predict its material
    properties.

# Inputs:

**Metagen Program:**

{code}

**Rendered Views:**
- Top: <[{top}]>
- Front: <[{ front }]>
- Right: <[{ right }]>
- Angled (Front-Top-Right): <[{ top_right }]>

# Output Format:

Output a json object, delimited by ```json ```, where the keys are material property names, and
    the values are the predicted material properties. Predict these properties (keys):
- "A" : Anisotropy ( universal anisotropy index)
- "E" : Young's Modulus relative to E_base
- "K" : Bulk modulus relative to E_base
- "G": Shear modulus relative to E_base
- "nu": Isotropic Poisson ratio
- "V" : Relative Density (Volume Fraction)
```